Title

MyD88-dependent interplay between myeloid and endothelial cells in the initiation and progression of obesity-associated inflammatory diseases.

Journal

The Journal of experimental medicine, 211(5)

ISSN

0022-1007

Authors

Yu, Minjia
Zhou, Hao
Zhao, Junjie
et al.

Publication Date

2014-05-01

DOI

10.1084/jem.20131314

Peer reviewed

MyD88-dependent interplay between myeloid and endothelial cells in the initiation and progression of obesity-associated inflammatory diseases

Minjia Yu,[1,6] Hao Zhou,[1,7] Junjie Zhao,[1] Nengming Xiao,[1] Sanjoy Roychowdhury,[3] David Schmitt,[2] Bingqing Hu,[1] Richard M. Ransohoff,[5] Clifford V. Harding,[9] Amy G. Hise,[9,10] Stanley L. Hazen,[2] Anthony L. DeFranco,[8] Paul L. Fox,[2] Richard E. Morton,[2] Paul E. Dicorleto,[2] Maria Febbraio,[4] Laura E. Nagy,[3] Jonathan D. Smith,[2] Jian-an Wang,[6] and Xiaoxia Li[1]

[1]Department of Immunology, [2]Department of Cellular and Molecular Medicine, [3]Department of Pathobiology, [4]Department of Molecular Cardiology, and [5]Department of Neurosciences, Cleveland Clinic, Cleveland, OH 44195
[6]Department of Cardiology, Second Affiliated Hospital, School of Medicine, Zhejiang University, Hangzhou, Zhejiang, 310009, China
[7]Department of Biological, Geological, and Environmental Sciences, Cleveland State University, Cleveland, OH 44115
[8]Department of Microbiology and Immunology, University of California, San Francisco, San Francisco, CA 94143
[9]Department of Pathology, Case Western Reserve University/University Hospitals Case Medical Center, Cleveland, OH 44106
[10]Center for Global Health and Diseases, Case Western Reserve University, School of Medicine, Cleveland, OH 44106

Low-grade systemic inflammation is often associated with metabolic syndrome, which plays a critical role in the development of the obesity-associated inflammatory diseases, including insulin resistance and atherosclerosis. Here, we investigate how Toll-like receptor–MyD88 signaling in myeloid and endothelial cells coordinately participates in the initiation and progression of high fat diet–induced systemic inflammation and metabolic inflammatory diseases. MyD88 deficiency in myeloid cells inhibits macrophage recruitment to adipose tissue and their switch to an M1-like phenotype. This is accompanied by substantially reduced diet-induced systemic inflammation, insulin resistance, and atherosclerosis. MyD88 deficiency in endothelial cells results in a moderate reduction in diet-induced adipose macrophage infiltration and M1 polarization, selective insulin sensitivity in adipose tissue, and amelioration of spontaneous atherosclerosis. Both in vivo and ex vivo studies suggest that MyD88-dependent GM-CSF production from the endothelial cells might play a critical role in the initiation of obesity-associated inflammation and development of atherosclerosis by priming the monocytes in the adipose and arterial tissues to differentiate into M1-like inflammatory macrophages. Collectively, these results implicate a critical MyD88-dependent interplay between myeloid and endothelial cells in the initiation and progression of obesity-associated inflammatory diseases.

CORRESPONDENCE
Xiaoxia Li E-mail:
lix@ccf.org

Abbreviations used: ATM, adipose tissue macrophage; BMDM, BM-derived macrophage; CLS, crownlike structure; GTT, glucose tolerance test; HFD, high-fat diet; PI3K, phosphoinositide 3 kinase.

The metabolic syndrome is characterized by a cluster of physiological alterations including glucose intolerance/insulin resistance, abdominal obesity, atherogenic dyslipidemia (low concentration of plasma high-density lipoprotein cholesterol and high concentration of plasma triglycerides), and elevated blood pressure. Occurring together, these conditions increase the risk for atherosclerosis and type 2 diabetes mellitus, which are typical obesity-associated diseases that are endemic in developed countries, currently affecting 25% of the population and growing (McCullough, 2011). Recent investigations have increasingly shown that low-grade systemic inflammation is often associated with metabolic syndrome, which probably plays a critical role in the development of these metabolic diseases

M. Yu and H. Zhou contributed equally to this paper.

The Rockefeller University Press $30.00
J. Exp. Med. 2014 Vol. 211 No. 5 887-907
www.jem.org/cgi/doi/10.1084/jem.20131314

The Journal of Experimental Medicine

(Hirosumi et al., 2002; Zieske et al., 2005; Hotamisligil, 2006; Wärnberg et al., 2006). Previous studies have shown that a high-fat diet (HFD) can increase the gut permeability, triggering the accumulation of systemic inflammatory stimuli (Erridge, 2011), including pathogen-associated molecular patterns, such as ligands for TLRs, endogenous TLR ligands such as fatty acids and inflammatory cytokines, including IL-1 (Shi et al., 2006; Cani et al., 2007; Creely et al., 2007; Cani et al., 2008; Holvoet et al., 2008; Dasu et al., 2012). Although inflammation is generally considered to be a localized reaction, it is now understood that a systemic inflammatory response can occur when inflammatory stimuli gain access to the circulation (Hotamisligil, 2006).

Genetic studies and mouse disease models have shown the participation of TLR and IL-1R in the development of HFD-induced systemic inflammation and obesity-associated inflammatory diseases. TLR4 deficiency reduced diet-induced insulin resistance and systemic inflammation (Shi et al., 2006), whereas TLR2-deficient mice were partially protected from diet-induced obesity (Himes and Smith, 2010). Human TLR4-null mutations are associated with reduced risk of atherosclerosis (Kiechl et al., 2002). ApoE$^{-/-}$ mice, a commonly used model, spontaneously develop atherosclerosis; deficiency in TLR4, IL-1, and IL-1R each reduced vascular inflammation and atherosclerosis in ApoE$^{-/-}$ mice (Kirii et al., 2003; Björkbacka et al., 2004; Chi et al., 2004; Michelsen et al., 2004). These previous studies suggested that exogenous/endogenous TLR ligands and the proinflammatory cytokine IL-1 can activate IL-1R/TLRs in multiple tissues, including adipose, liver, pancreas, aorta, heart, and muscle. As a consequence, a chronic systemic inflammatory response is established, which is strongly associated with the development of type II diabetes and atherosclerosis (Erridge, 2011; Fresno et al., 2011; Könner and Brüning, 2011). Much effort has been devoted toward the understanding of IL-1R/TLR-mediated signaling mechanisms, with the long-term objective to identify new therapeutic targets and develop more effective antiinflammatory small molecule drugs. Upon ligand stimulation, IL-1R and TLRs form either homo- or hetero-oligomers. The adapter molecule MyD88 is recruited to all IL-1R/TLR oligomers, with the exception of TLR3, followed by the recruitment of the serine/threonine IL-1 receptor kinases (IRAKs; Takeuchi and Akira, 2002; Kenny and O'Neill, 2008; Lin et al., 2010; Brown et al., 2011; Gay et al., 2011). Genetic and biochemical studies revealed that through activation of MyD88-IRAKs, downstream kinases are organized by multiple adapter molecules into parallel and sequential signaling cascades, leading to activation of the transcription factor NF-κB and mitogen-activated protein kinases (Kim et al., 2007; Yao et al., 2007; Fraczek et al., 2008), resulting in the production of inflammatory cytokines and chemokines.

Although TLR-MyD88 signaling has been implicated in obesity-associated inflammatory diseases, the molecular and cellular mechanisms are not completely understood. In this study, we investigated how TLR-MyD88 signaling in different cellular compartments coordinately participates in the initiation of HFD-induced systemic inflammation and metabolic inflammatory diseases. The cell type–specific MyD88$^{-/-}$ mice are crucial, as complete MyD88$^{-/-}$ mice (1) are immune compromised and prone to infection; (2) do not adequately reflect specific role of MyD88 in different cell types (Subramanian et al., 2013). Indeed, several previous studies using complete MyD88$^{-/-}$ mice produced conflicting results regarding the role of MyD88 in obesity-associated inflammatory diseases, which might be due to the immune deficiency of complete MyD88$^{-/-}$ mice and the housing environment in different institutions (Björkbacka et al., 2004; Michelsen et al., 2004; Hosoi et al., 2010). Therefore, studies using cell type–specific MyD88$^{-/-}$ mice are necessary and timely to elucidate the mechanistic role of TLR-MyD88 signaling in obesity-associated inflammatory diseases.

Using cell type–specific MyD88-deficient mice, our findings for the first time demonstrate the MyD88-dependent cooperative actions of myeloid and endothelial cells in the development and progression of metabolic inflammatory diseases. MyD88 deficiency in myeloid cells (MyD88$^{MC\text{-}KO}$) substantially reduced diet-induced systemic inflammation, insulin resistance, and atherosclerosis. Furthermore, deletion of MyD88 in myeloid cells prevented macrophage infiltration into adipose tissue and aborted a switch in adipose tissue macrophage (ATM) phenotype from M2-like to M1-like. Using an adipocyte-macrophage ex vivo co-culture system and adipocyte-derived endogenous TLR ligand FFA, we demonstrated the influence of adipocytes on MyD88-dependent induction of M1-associated genes in macrophages, indicating the cross-talk between adipocytes and macrophages. On the other hand, MyD88 deficiency in endothelial cells (MyD88$^{EC\text{-}KO}$) showed moderate reduction in diet-induced adipose M1-like macrophages with selective insulin sensitivity in adipose tissue, and amelioration of spontaneous atherosclerosis. Both in vivo and ex vivo studies suggest that MyD88-dependent GM-CSF production from the endothelial cells might play a critical role in the initiation of obesity-associated inflammation and development of atherosclerosis by priming the monocytes in the adipose and arterial tissues to M1-like inflammatory macrophages. Collectively, these results implicate a critical MyD88-dependent interplay among adipocytes, macrophages, and endothelial cells in the initiation of diet-induced systemic inflammatory state and metabolic diseases.

RESULTS

Generation of myeloid- and endothelial cell–specific MyD88-deficient mice

Endothelial cell–specific MyD88-deficient mice created by cre-lox technology were validated by PCR (Fig. 1 A) and Western-blot analysis (not depicted). Tie2eCre transgenic mice (generated using the Tie2 5′ promoter and first intron enhancer element) express Cre within endothelium of brain, heart, and liver, among others (Kano et al., 2003; Kang et al., 2010). It is important to note that Tie2eCre (distinct from Tie2Cre) is restricted to endothelium, and Cre expression is minimally leaky (Kano et al., 2003; Kang et al., 2010). MyD88 expression was abolished in CD31^{+} endothelial cells from the

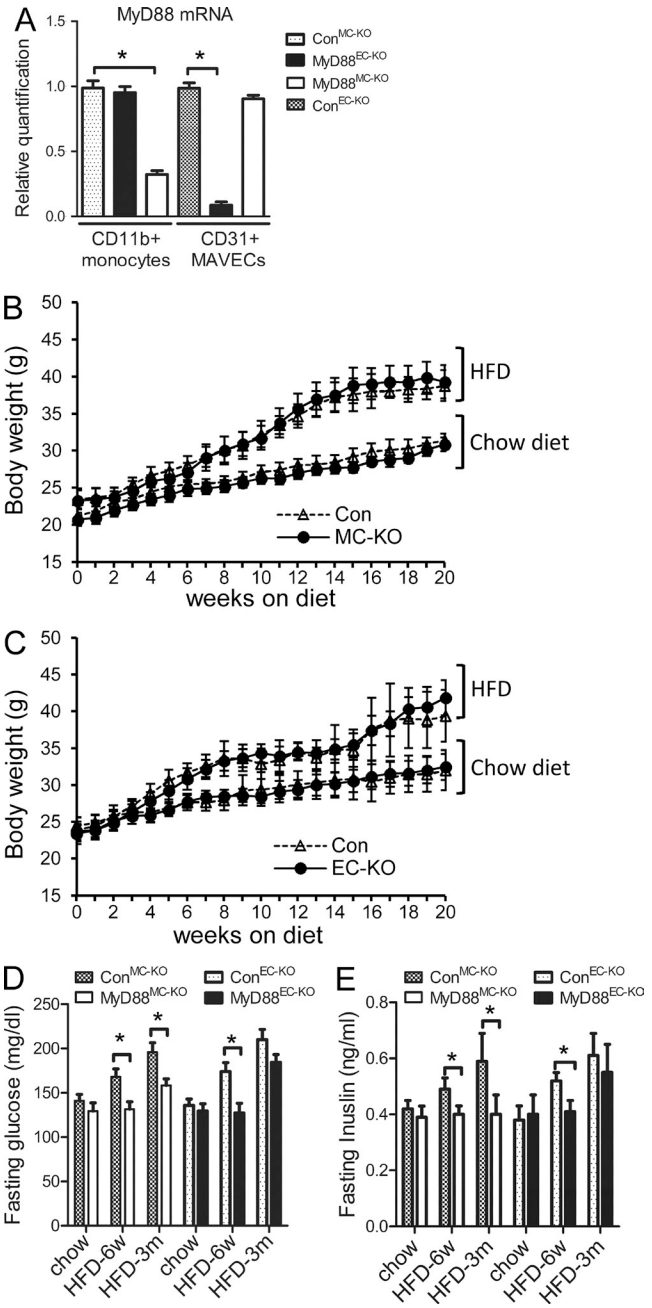

Figure 1. MyD88 deficiency in myeloid and endothelial cells improves diet-induced hyperglycemia and hyperinsulinemia. (A) PCR for MyD88 mRNA of mouse CD11b$^+$ splenic monocytes (CD11b$^+$ monocytes) and CD31$^+$ primary aortic vascular endothelial cells (MAVECs) from MyD88$^{EC\text{-}KO}$, MyD88$^{MC\text{-}KO}$ and their respective littermate controls (Con$^{MC\text{-}KO}$ and Con$^{EC\text{-}KO}$). Data are presented as mean ± SD based on 5–7 for each group and are representative of three independent experiments. Body weights of (B) MyD88$^{MC\text{-}KO}$ or (C) MyD88$^{EC\text{-}KO}$ male mice and their littermate controls (maintained on a chow diet or HFD) were measured weekly from 6–26 wk of age. (D) Serum fasting glucose and (E) fasting insulin levels were measured in MyD88$^{MC\text{-}KO}$, MyD88$^{EC\text{-}KO}$ male mice and their respective littermate controls fed on chow diet (6 mo of age) or HFD (for 6 wk or 3 mo starting from 6 wk of age). n = 9–11 mice per genotype. Data are representative of two independent experiments. *, $P < 0.05$.

aortas of Tie2eCreMyD88$^{fl/fl}$ (MyD88$^{EC\text{-}KO}$) mice compared with control (Tie2eCreMyD88$^{fl/+}$, Con $^{EC\text{-}KO}$), but showed normal MyD88 expression in monocytes (Fig. 1 A). To generate myeloid-specific MyD88-deficient mice, we used CD11bCre transgenic mice (generated with the promoter for CD11b, an integrin expressed exclusively in the myeloid lineage; Boillée et al., 2006; Kang et al., 2010; Kang et al., 2012). These mice express Cre in macrophages, microglia, and activated liver Kupffer cells. CD11bCreMyD88$^{fl/+}$ mice were bred to MyD88$^{fl/fl}$ to generate control mice (CD11bCreMyD88$^{fl/+}$, Con$^{MC\text{-}KO}$) and myeloid-specific MyD88-deficient mice (CD11bCreMyD88$^{fl/fl}$, MyD88$^{MC\text{-}KO}$). PCR analysis showed that MyD88 expression was diminished in CD11b$^+$ monocytes derived from CD11bCreMyD88$^{fl/fl}$ (MyD88$^{MC\text{-}KO}$) mice compared with that in Con$^{MC\text{-}KO}$ mice (Fig. 1 A).

MyD88 deficiency in myeloid and endothelial cells reduce diet-induced insulin resistance

We first analyzed metabolic parameters of MyD88$^{MC\text{-}KO}$ and MyD88$^{EC\text{-}KO}$ mice on chow diet or HFD. There were no substantial differences in weight gain over the course of 20 wk (Fig. 1, B and C) with similar levels of serum cholesterol, triglycerides, and nonesterified fatty acids (not depicted) in MyD88$^{MC\text{-}KO}$ and MyD88$^{EC\text{-}KO}$ mice fed on chow or HFD compared with their respective littermate controls. These results indicate that MyD88 deficiency in endothelial or myeloid cells did not affect diet-induced weight gain and lipid homeostasis. We then examined glucose metabolism in the MyD88$^{MC\text{-}KO}$ and MyD88$^{EC\text{-}KO}$ mice. Interestingly, after HFD (for 6 wk and 3 mo), fasting glucose and fasting insulin levels were substantially decreased in MyD88$^{MC\text{-}KO}$ mice compared with the littermate controls (Fig. 1, D and E). By performing a glucose tolerance test (GTT), we found that HFD-fed MyD88$^{MC\text{-}KO}$ mice had much improved glucose tolerance compared with the littermate controls (Fig. 2, A and B). Endothelial MyD88 deficiency also improved insulin sensitivity, but the impact was more dramatic at early phase (6 wk) compared with that after 3 mo of HFD (Fig. 2, C and D). As controls, we noticed that the glucose tolerance and insulin sensitivity in chow diet–fed MyD88$^{MC\text{-}KO}$ and MyD88$^{EC\text{-}KO}$ mice were comparable with their respective littermate controls (Fig. 1, D and E; and not depicted).

Deletion of MyD88 in myeloid cells and endothelial cells preserves insulin signaling in different tissues

Because MyD88 deficiency in myeloid and endothelial cells attenuated diet-induced insulin resistance, we next examined insulin sensitivity in several tissues (including adipose tissue, muscle, and liver) by i.p. injecting HFD-fed mice with insulin or saline after an overnight fast. As expected, compared with normal chow-fed mice, insulin-induced AKT phosphorylation, tyrosine phosphorylation of IRS1 (insulin receptor substrate 1), and IRS1 interaction with p85-phosphoinositide 3 kinase (PI3K) were greatly reduced in adipose tissue, liver, and muscle of HFD-fed wild-type control mice (Fig. 3, A–D), demonstrating diet-induced insulin insensitivity of these tissues. Interestingly, although insulin-induced AKT phosphorylation was

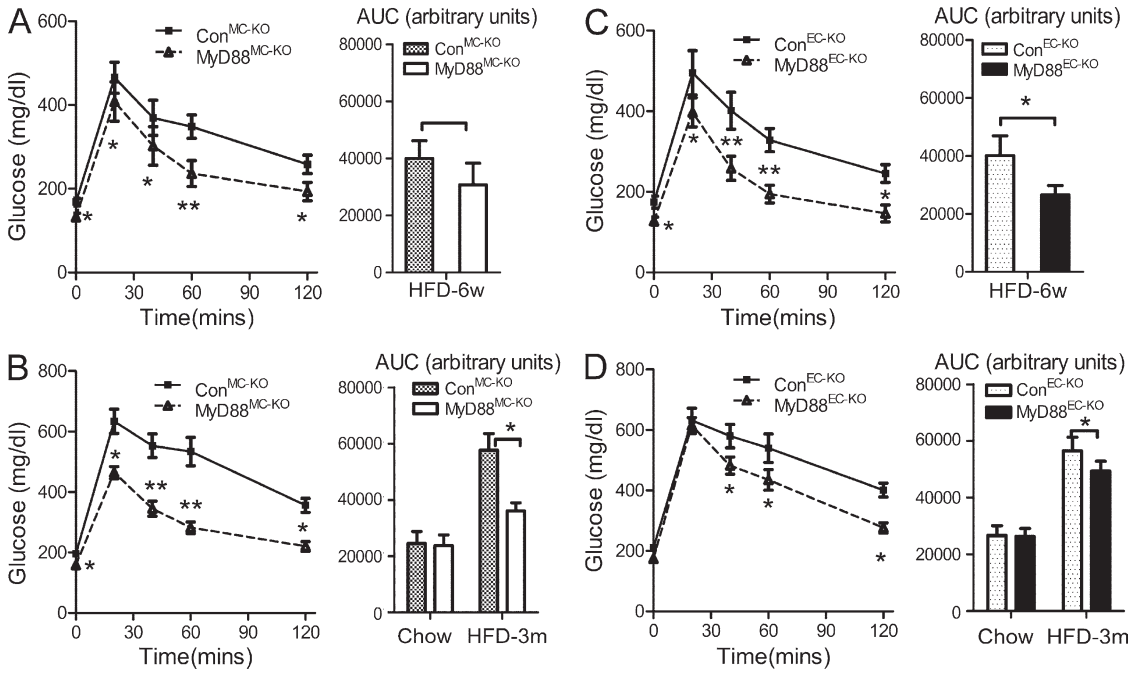

Figure 2. Deletion of MyD88 in myeloid cells and endothelial cells reduces diet-induced insulin resistance. GTTs in MyD88^{MC-KO} male mice and littermate controls on HFD for (A) 6 wk or (B) 3 mo starting from 6-wk-old (6-mo-old mice on chow diet as controls, data not shown). Area under curve (AUC) was calculated. GTT in MyD88^{EC-KO} mice and their littermate controls on HFD for (C) 6 wk or (D) 3 mo starting from 6 wk of age (6-mo-old mice on chow diet as controls, data not shown). AUC was calculated. Data are presented as mean ± SEM (n = 9–11 mice per genotype) and are representative of two independent experiments. *, $P < 0.05$; **, $P < 0.01$.

preserved in all three tissues of HFD-fed MyD88^{MC-KO} mice, endothelial-specific MyD88 deficiency only rescued insulin signaling substantially in adipose tissue(Fig. 3, E–H). Consistently, insulin-induced IRS-1 tyrosine phosphorylation and its association with PI3K (p85) were preserved in adipose tissue, liver, and muscle of HFD-fed MyD88^{MC-KO} mice, but only restored in adipose tissue of HFD-fed MyD88^{EC-KO} mice, compared with that in their respective HFD-fed littermate controls (Fig. 3, E–H). Thus, endothelial-derived MyD88 plays a more important role in HFD-induced insulin resistance in the adipose tissue than that in liver and muscle.

Myeloid- and endothelial-specific MyD88 deficiency protect mice from atherosclerosis in ApoE$^{-/-}$ mice

Atherosclerosis is a chronic inflammatory disease of the arteries, representing the underlying cause of the majority of cardiovascular disease. Obesity is an independent risk factor for the development of cardiovascular atherosclerosis. Obesity-induced insulin resistance and impaired glucose metabolism can exacerbate atherosclerosis. To study the impact of MyD88 deficiency in endothelial or myeloid cells on the pathogenesis of atherosclerosis, we used the ApoE-deficient mice, which spontaneously develop hypercholesterolemia and atherosclerosis. Because female ApoE$^{-/-}$ mice were shown to develop a more severe phenotype than male ApoE$^{-/-}$(Caligiuri et al., 1999; Smith et al., 2010), we decided to use the female mice in this model. MyD88^{MC-KO}, MyD88^{EC-KO} mice, and respective littermate controls were crossed to ApoE$^{-/-}$ mice to generate MyD88^{MC-KO}ApoE$^{-/-}$, MyD88^{EC-KO}ApoE$^{-/-}$ mice and control mice (Con^{MC-KO}ApoE$^{-/-}$ and Con^{EC-KO}ApoE$^{-/-}$ mice). Total plasma cholesterol levels and cholesterol distribution were similar among 18-wk-old female MyD88^{MC-KO}ApoE$^{-/-}$, MyD88^{EC-KO} ApoE$^{-/-}$ and their respective littermate controls either on chow diet or HFD (unpublished data).

We first compared the severity of atherosclerosis in chow-fed MyD88^{MC-KO}ApoE$^{-/-}$, MyD88^{EC-KO}ApoE$^{-/-}$ and their respective littermate controls at 18 wk of age. En face and aortic root section analysis of atherosclerotic lesions showed ~60–70% reduction in both MyD88^{MC-KO} ApoE$^{-/-}$ and MyD88^{EC-KO} ApoE$^{-/-}$ mice compared with littermate controls (Fig. 4, A–D). Thus, MyD88 deficiency in endothelial or myeloid cells inhibited vascular lesion formation in this model of spontaneous atherosclerosis. Consistently, under chow diet MyD88 deficiency in myeloid or endothelial cells had similar impact on insulin sensitivity of aortas compared with that in their littermate controls (Fig. 4 E). We next examined expression of inflammatory genes in arterial tissue of both MyD88^{MC-KO} ApoE$^{-/-}$ and MyD88^{EC-KO}ApoE$^{-/-}$mice. The expression levels of M-CSF, MCP-1, iNOS, VCAM-1, ICAM-1, and especially GM-CSF, were substantially reduced in the arterial tissue of MyD88 $^{EC-KO}$ApoE$^{-/-}$mice, whereas TNF, IL-6 and IL-1 were similarly decreased in arterial tissue of MyD88^{EC-KO} ApoE$^{-/-}$ and MyD88^{MC-KO}ApoE$^{-/-}$ mice compared with that of littermate controls (Fig. 5, A and B).

Because it is well known that the pathology of atherosclerosis in ApoE$^{-/-}$ mice is further aggravated upon HFD feeding,

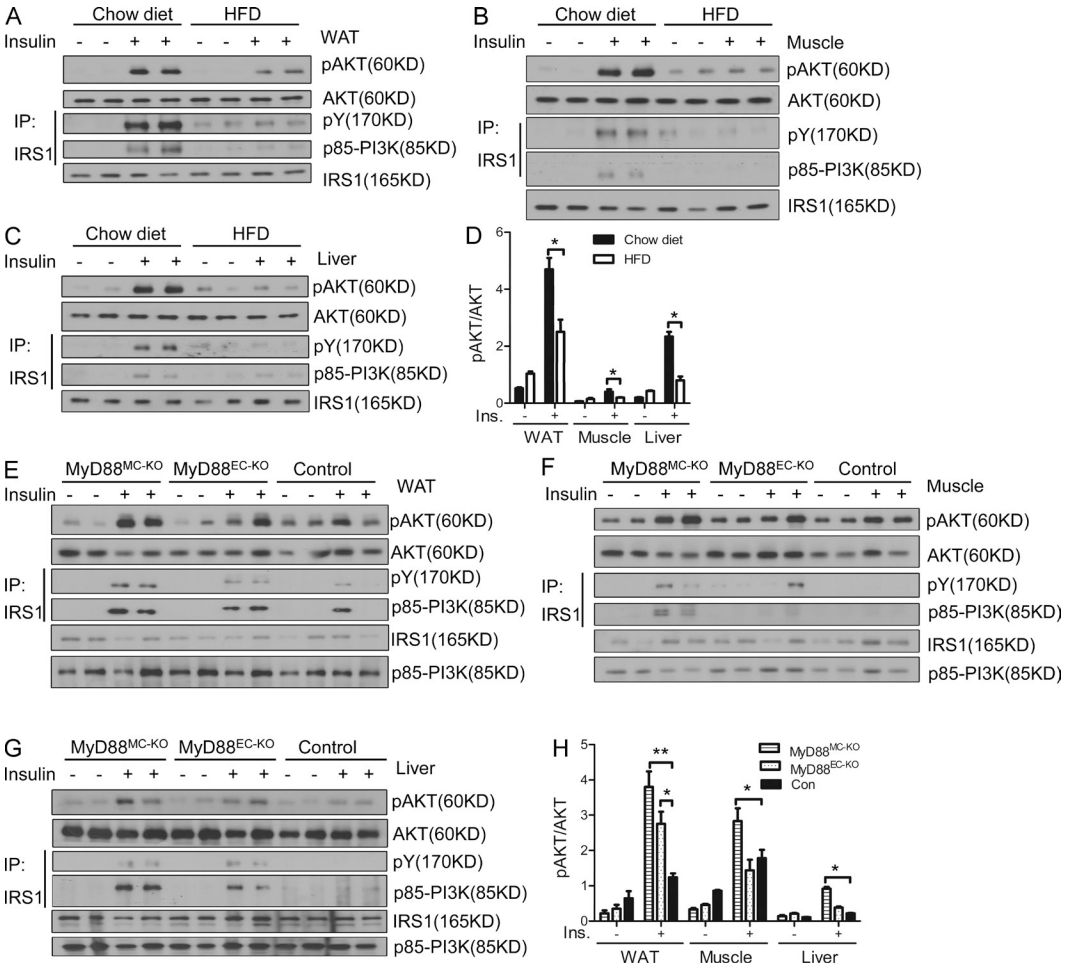

Figure 3. Deletion of MyD88 in myeloid cells and endothelial cells preserves insulin signaling. After overnight fast, 5-mo-old control group (CD11bCreMyD88$^{fl/+}$ and Tie2eCreMyD88$^{fl/+}$) male mice kept on chow diet or HFD were injected with either saline (−) or 25 mU/kg of insulin (+). (A) White adipose tissues (WAT), (B) muscles, and (C) livers were collected 5 min later. (E) WAT, (F) muscles, and (G) livers of MyD88^{MC-KO}, MyD88^{EC-KO}, and control group male mice kept on HFD for 3 mo were collected at 5 min after saline or insulin injection. Protein extracts were prepared, immunoprecipitated with anti-IRS-1, followed by Western blot analysis with antibodies for phosphotyrosine (PY20, pY) or p85-PI3K. The levels of IRS1, activated AKT (pSer473, pAKT) and total AKT, were determined by immunoblotting of the original lysates. (D and H) The levels of pAKT and AKT were quantified by densitometry. The ratio of pAKT to AKT was expressed as a mean ± SEM (*, $P < 0.05$; **, $P < 0.01$). $n = 4$ mice per genotype. The results are representative of three independent experiments.

we then compared diet-induced atherosclerotic lesions of the endothelial- and myeloid-specific MyD88-deficient mice with their littermate controls. En face and aortic root section analysis of atherosclerotic lesions showed ∼70% versus 40% reduction, respectively, in lesion areas of MyD88^{MC-KO} ApoE$^{-/-}$ mice and MyD88^{EC-KO} ApoE$^{-/-}$ mice compared with their littermate controls (Fig. 4, A–D). It is important to note that HFD substantially induced insulin resistance in the aortas of wild-type control mice. Both MyD88^{MC-KO} ApoE$^{-/-}$ and MyD88^{EC-KO} ApoE$^{-/-}$ mice showed improved insulin sensitivity of aortas compared with their littermate controls (Fig. 4 E). The expression of inflammatory genes (CXCL1, TNF, IL-6, and IL-1) was more dramatically decreased in arterial tissue of MyD88^{MC-KO} ApoE$^{-/-}$ than that in MyD88^{EC-KO} ApoE$^{-/-}$mice compared with their respective littermate controls (Fig. 5, C and D). On the other hand, the expression of several inflammatory genes (M-CSF, MCP-1, iNOS, VCAM-1, and ICAM-1) was equally decreased in arterial tissue of MyD88^{MC-KO} ApoE$^{-/-}$ and MyD88^{EC-KO}ApoE$^{-/-}$mice compared with littermate controls (Fig. 5, C and D). It is important to note that the expression of GM-CSF was more dramatically decreased in arterial tissue of MyD88^{EC-KO} ApoE$^{-/-}$ than that in MyD88^{MC-KO}ApoE$^{-/-}$mice compared with that in littermate controls (Fig. 5, C and D). Lastly, through the analysis of gene expression in aorta, we did notice that the expression of Arg1 and IL-10 were always enhanced in the arterial tissue of either chow- or HFD-fed MyD88^{EC-KO} ApoE$^{-/-}$ and MyD88^{MC-KO}ApoE$^{-/-}$ mice compared with that in their respective littermate controls (Fig. 5, A–D), which will be further discussed below.

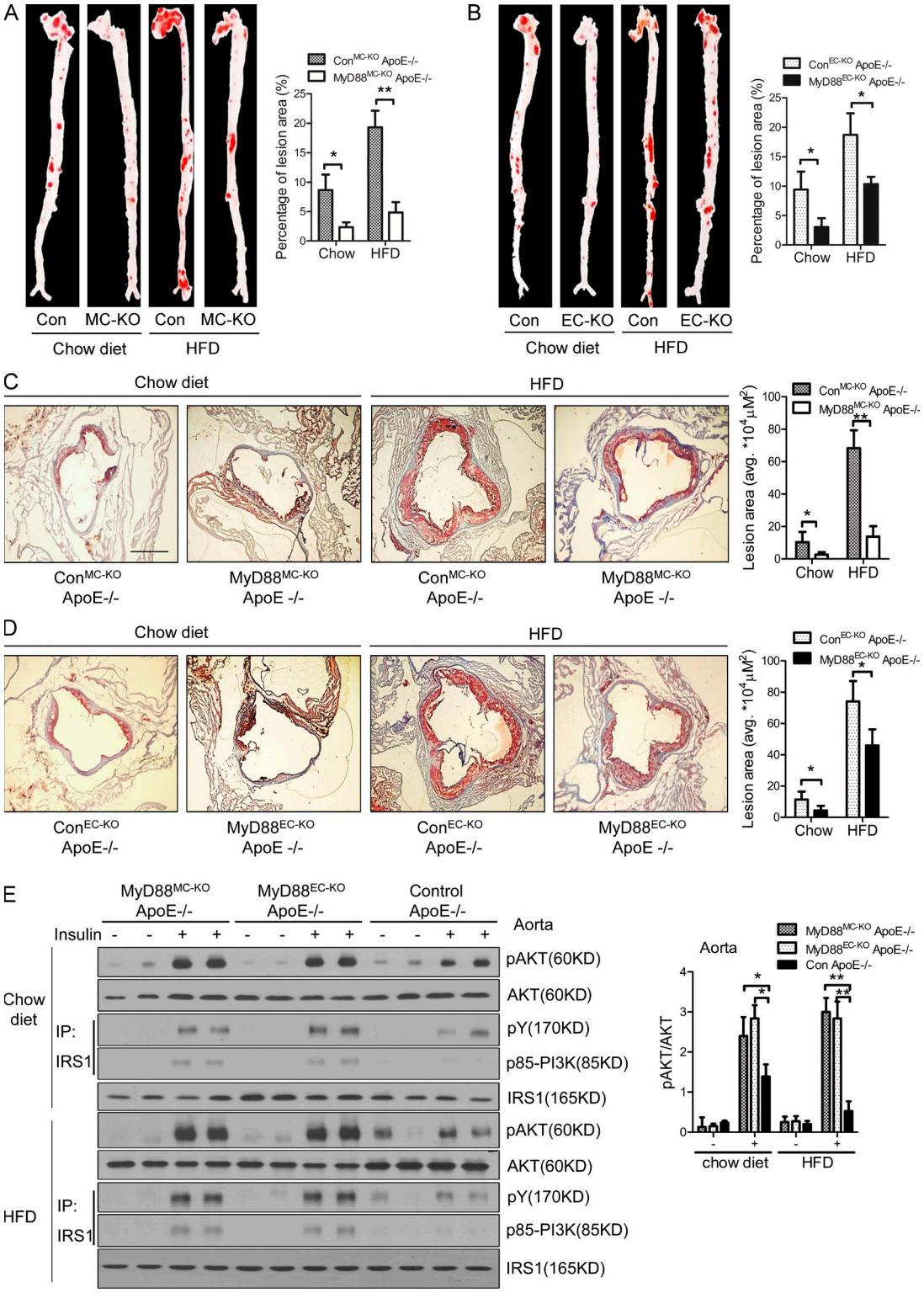

Figure 4. Myeloid- and endothelial-specific MyD88 deficiency protect mice from atherosclerosis. (A) MyD88^{MC-KO} ApoE$^{-/-}$ and (B) MyD88^{EC-KO} ApoE$^{-/-}$ female mice and their respective littermate controls (Con^{MC-KO} ApoE$^{-/-}$ and Con^{EC-KO} ApoE$^{-/-}$), were fed on chow diet or HFD for 12 wk beginning at 6 wk of age. Enface (oil red O staining) analysis was done for the whole aorta tree from end of the curvature of the aortic arch to the iliac bifurcation from these mice. Total mean lesion area was quantified based on image-analysis (Photoshop; Adobe). Data are presented as mean ± SEM (n = 9–12 mice per genotype) and are representative of two independent experiments. *, P < 0.05; **, P < 0.01. Cross-sections of aortic roots from (C) MyD88^{MC-KO} ApoE$^{-/-}$ and (D) MyD88^{EC-KO} ApoE$^{-/-}$ female mice and their respective littermate controls fed on chow diet or HFD for 12 wk were stained with oil red O

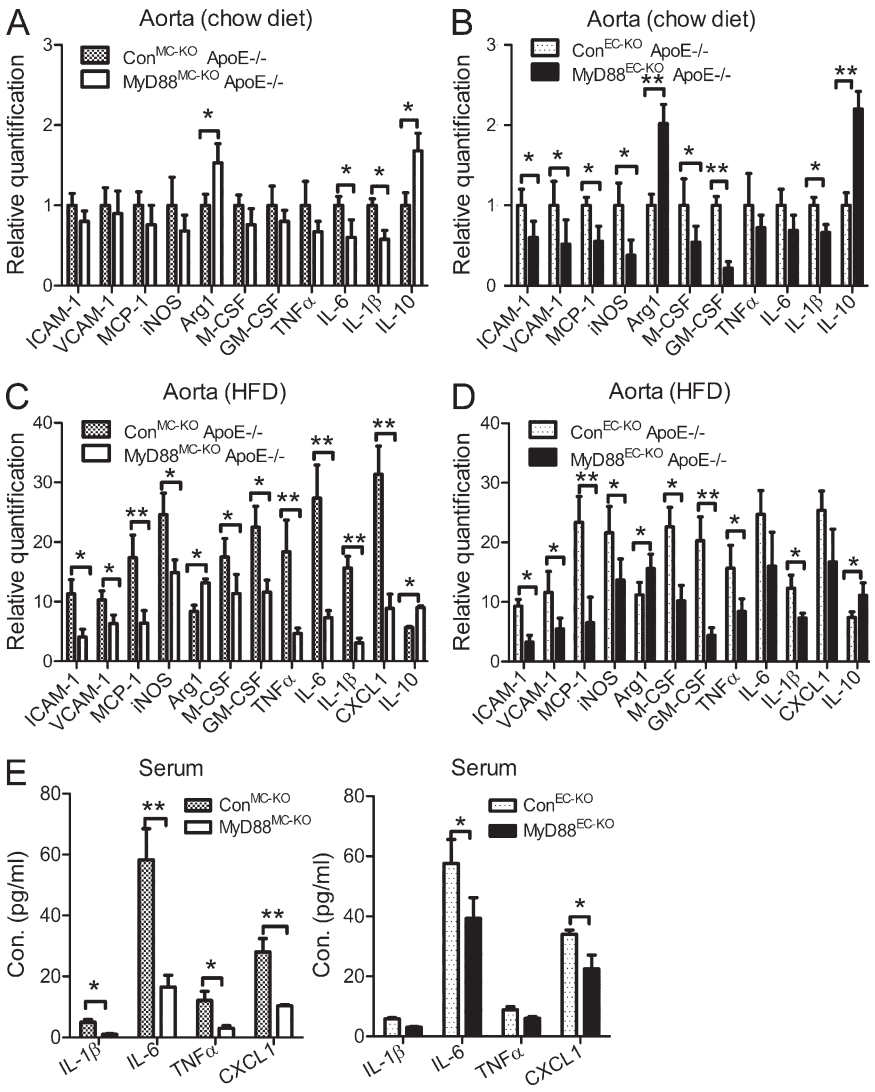

Figure 5. MyD88 deficiency in myeloid and endothelial cells ameliorates arterial tissue inflammation under hypercholesterolemia and diet-induced systemic inflammation. Total RNA of aortas was isolated from MyD88$^{MC\text{-}KO}$ ApoE$^{-/-}$ female mice and littermate control mice on chow diet (A) or HFD (C); MyD88$^{EC\text{-}KO}$ ApoE$^{-/-}$ female mice and their respective littermate controls on chow diet (B) or HFD (D); and followed by quantitative real-time PCR and normalized to β-actin for the indicated genes. The mean value of each gene in control groups on chow diet was set to 1. The mean value of each gene in mice on HFD was normalized to that in their respective controls on chow diet. Data are presented as mean ± SEM (n = 9–12 mice per genotype) and are representative of two independent experiments. (E) Protein levels of IL-1β, IL-6, TNF, and CXCL1 in the serum from MyD88$^{MC\text{-}KO}$ ApoE$^{-/-}$, MyD88$^{EC\text{-}KO}$ ApoE$^{-/-}$ female mice and their respective littermate controls were analyzed by ELISA. n = 7–9 mice per genotyping. Data are presented in F–J as mean ± SEM. *, P < 0.05; **, P < 0.01. The results are representative of two independent experiments.

Myeloid-derived MyD88 is required for HFD-induced systemic inflammation

Recent studies have shown a direct link between "chronic systemic inflammation" and diet-induced metabolic syndrome and consequent obesity-associated inflammatory diseases (Elhage et al., 1998; Huber et al., 1999; Cheung et al., 2000; Klover et al., 2003; Plomgaard et al., 2005; Hotamisligil, 2006; De Taeye et al., 2007; Dixon and Symmons, 2007; Avouac and Allanore, 2008; Kleemann et al., 2008; Ehses et al., 2009; Ferrante et al., 2009; Monteiro and Azevedo, 2010; Emanuela et al., 2012). Low-grade inflammation triggered by the HFD was indeed detected in the circulation of control mice, whereas diet-induced serum proinflammatory cytokines (IL-1, IL-6, TNF, and CXCL1) were greatly reduced in MyD88$^{MC\text{-}KO}$ mice (Fig. 5 E). On the other hand, the deletion of MyD88 in endothelial cells only moderately reduced serum levels of these proinflammatory cytokines (Fig. 5 E). As shown in Fig. 4 (A–D), myeloid MyD88 also plays a more critical role than endothelial MyD88 in HFD-induced atherosclerosis, suggesting that systemic inflammation might contribute to HFD-induced exacerbation on atherosclerosis. Under systemic inflammation, in addition to ox-LDL and IL-1, the endothelium is probably also activated by other circulating inflammatory stimuli through MyD88-independent pathways, including TNF and IL-6 (Aird, 2007). Collectively, our results suggest that whereas both myeloid and endothelial MyD88 participate in the initiation of

(bar, 250 µm). Total mean lesion area was quantified by Photoshop software and shown as mean ± SEM and are representative of three independent experiments. *, P < 0.05; **, P < 0.01. n = 6–7 mice per genotype. (E) Aortas of MyD88$^{MC\text{-}KO}$ ApoE$^{-/-}$, MyD88$^{EC\text{-}KO}$ ApoE$^{-/-}$, and control group female mice kept on either chow diet or HFD for 3 mo were collected at 5 min after saline or insulin injection. Protein extracts were analyzed as described in Fig. 2 (A–D). The levels of pAKT and AKT were quantified by densitometry. The ratio of pAKT to AKT was expressed as a mean ± SEM. *, P < 0.05; **, P < 0.01. n = 4 mice per genotype. The results are representative of three independent experiments.

obesity-induced inflammatory diseases, myeloid MyD88 might play a more dominant role in disease progression through its impact on systemic inflammation.

Myeloid MyD88 participates in HFD-induced switching of ATM from M2-like to M1-like

Metabolic-triggered inflammation in white adipose tissue plays a key role in initiation of inflammatory diseases associated with metabolic syndrome, by directly impacting local and systemic insulin signaling and consequent long-term systemic inflammation (Hotamisligil et al., 1993; Xu et al., 2003; Neels and Olefsky, 2006; Nishimura et al., 2009; Wajchenberg et al., 2009). Obesity-induced adipose tissue inflammation is characterized by the presence of an increased number of adipose tissue–infiltrating macrophages (Weisberg et al., 2003). Compared with littermate controls, MyD88$^{MC\text{-}KO}$ mice showed

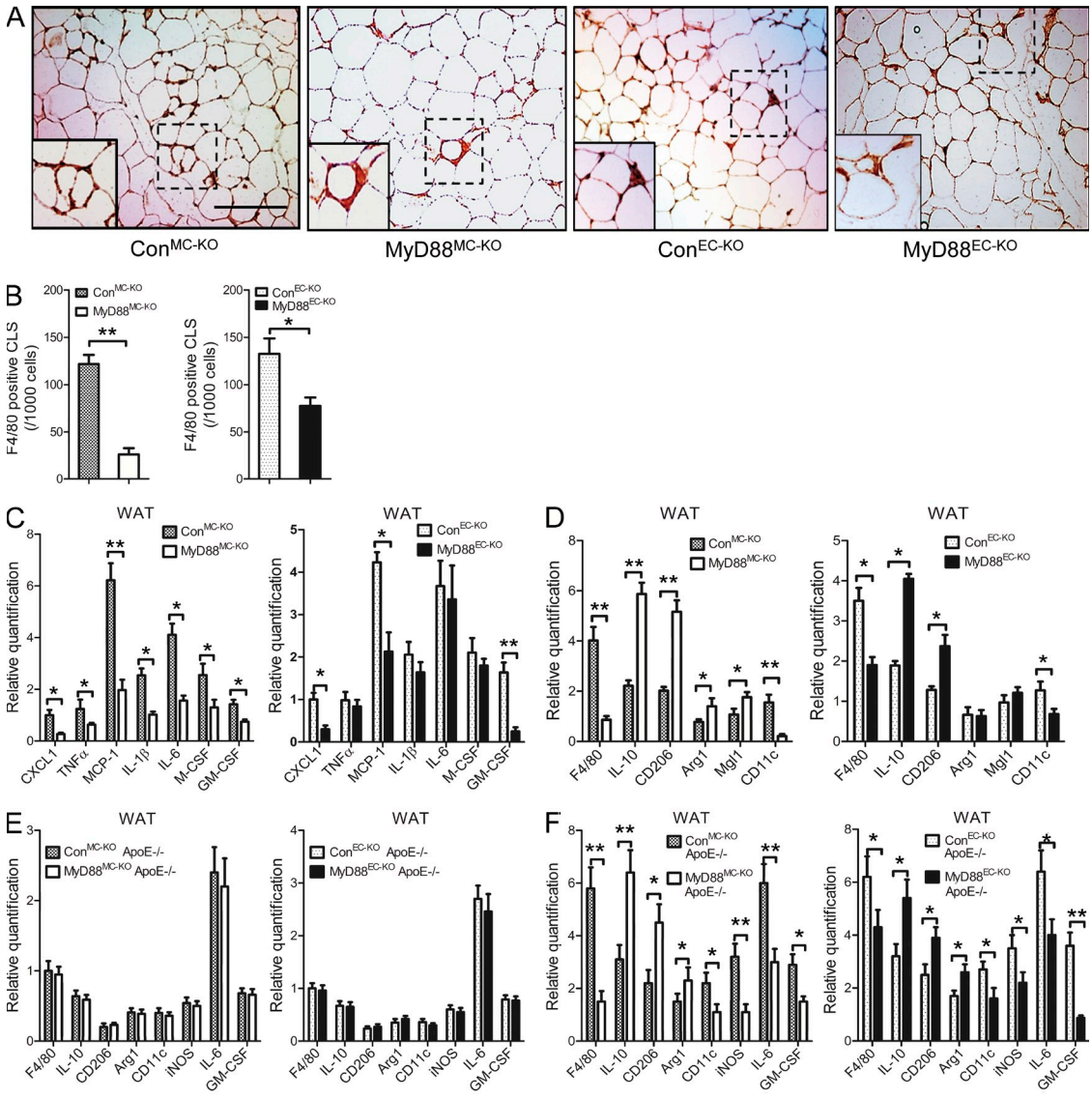

Figure 6. Deletion of MyD88 in myeloid cells and endothelial cells reduces diet-induced adipose tissue inflammation. MyD88$^{MC\text{-}KO}$, MyD88$^{EC\text{-}KO}$ male mice and their respective littermate controls on HFD for 14 wk were sacrificed and epididymal fat pad was collected. (A) Paraffin sections of epididymal fat pad were stained with anti-F4/80 antibody (bar, 50 µm). Arrowheads indicate F4/80$^+$ staining; representative CLSs were enlarged and shown in the insert. (B) The number of CLSs was counted. Results are shown as mean ± SEM of five different sections per mouse and are representative of five mice per genotype with similar results. The results are representative of two independent experiments. (C and D) Total adipose tissue RNA from MyD88$^{MC\text{-}KO}$, MyD88$^{EC\text{-}KO}$, and their respective littermate control mice were analyzed by quantitative real-time PCR and normalized to β-actin for the indicated genes. Data are presented as mean ± SEM (n = 9–11 per genotype) and are representative of two independent experiments. *, $P < 0.05$; **, $P < 0.01$. MyD88$^{MC\text{-}KO}$ ApoE$^{-/-}$, MyD88$^{EC\text{-}KO}$ ApoE$^{-/-}$ male mice and their respective littermate controls fed on either chow diet (E) or HFD (F) for 12 wk were sacrificed and epididymal fat pad was collected. Total adipose tissue RNA were analyzed by quantitative real-time PCR and normalized to β-actin for the indicated genes. Data are presented as mean ± SEM (n = 5–6 per genotype) and are representative of two independent experiments. *, $P < 0.05$; **, $P < 0.01$.

markedly reduced infiltration of macrophages and fewer so-called crownlike structures (CLSs), which are associated with inflammation and apoptotic/necrotic adipocytes (Fig. 6, A, B, and F4/80 levels in D). In support of the histology, mRNA expression levels of inflammatory genes were greatly decreased in adipose tissue of MyD88^{MC-KO} mice compared with controls (Fig. 6 C).

ATMs consist of at least two different phenotypes, classically activated M1-like macrophages and alternatively activated, resident M2-like macrophages. In obesity, infiltrating M1-like macrophages lead to an overall switch in adipose tissue phenotype, associated with insulin resistance and chronic inflammation (Weisberg et al., 2003; Xu et al., 2003; Lumeng et al., 2007; Zeyda and Stulnig, 2007; Fujisaka et al., 2009; Nguyen et al., 2007; Ohashi et al., 2010; Shaul et al., 2010; Zeyda et al., 2010; Prieur et al., 2011; Sun et al., 2011; Morris et al., 2012). Interestingly, we found that gene markers for M2-like macrophages, including IL-10, C-type mannose receptor 2 (CD206), Arginase-1, and macrophage galactose *N*-acetyl-galactosamine–specific lectin 1 (Mgl-1) were increased in adipose tissue of MyD88^{MC-KO}, whereas M1-like marker CD11c was decreased (Fig. 6 D), which is consistent with the improved adipose inflammatory status of these mice. When gated on CD11b$^+$F4/80$^+$ cells from adipose tissue of HFD-fed mice, the elimination of MyD88 in myeloid cells increased the number of M2-like macrophages (CD11c$^-$CD206$^+$) with decreased M1-like macrophages (CD11c$^+$CD206$^-$), confirming the critical role of MyD88-dependent signaling in HFD-induced ATM switching from M2- to M1-like macrophages (Fig. 7 A). We then sorted for M1-like (F4/80$^+$CD11c$^+$) and M2-like (F4/80$^+$CD206$^+$) macrophages from adipose tissues of HFD-fed MyD88^{MC-KO} and control mice, followed by gene expression analysis. Inflammatory gene expression (iNOS and IL-6) was much higher in M1-like than that in M2-like macrophages and substantially reduced in MyD88-deficient M1- and M2-like macrophages compared with their corresponding control macrophages, respectively (Fig. 7 B). On the other hand, M2-associated gene expression (Mgl1 and IL-10) was much higher in M2-like than that in M1-like macrophages and

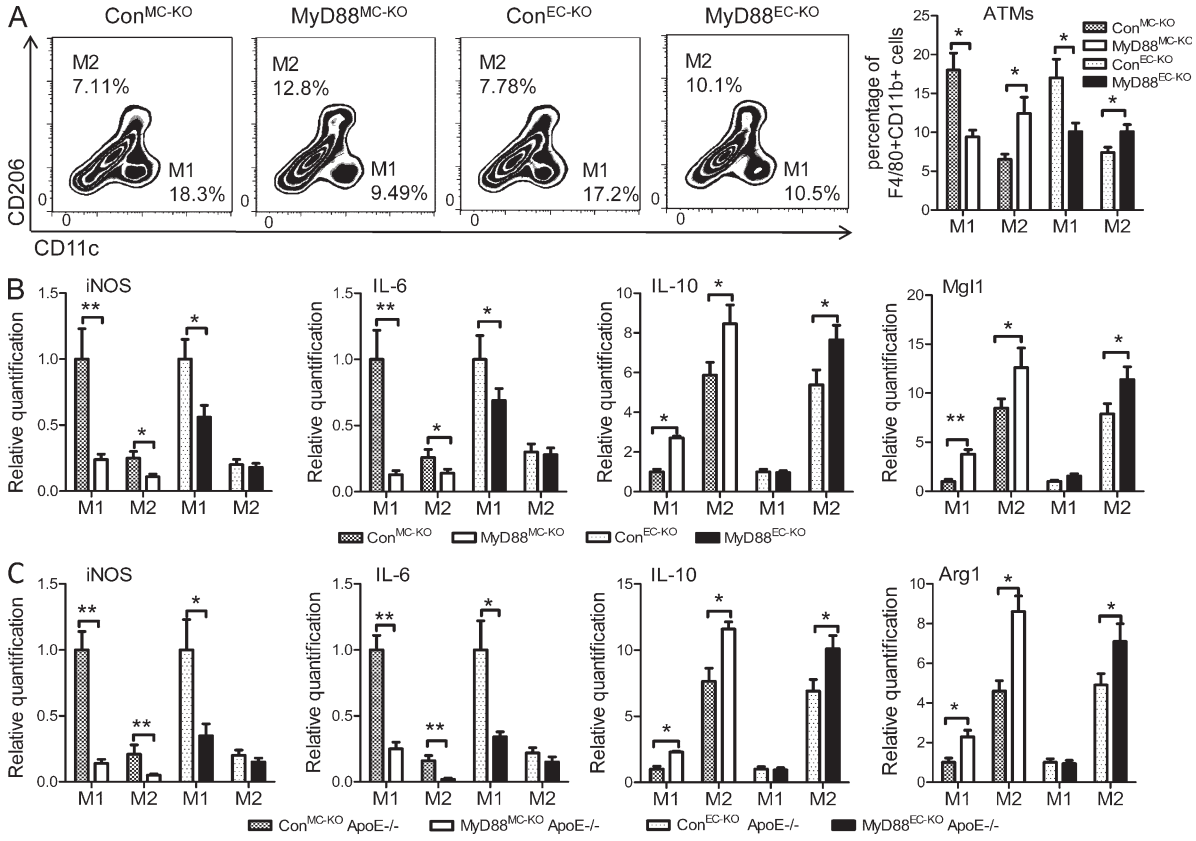

Figure 7. MyD88 participates in HFD-induced switching of ATM from M2 to M1. (A) Stromal vascular fraction (SVF) cells from epididymal fat pad of 6-mo-old MyD88^{MC-KO}, MyD88^{EC-KO} mice and their respective littermate controls on HFD were analyzed by flow cytometry. CD11b$^+$F4/80$^+$ (ATMs) were further analyzed with anti-CD11c and anti-CD206 antibodies. M1-like (F4/80$^+$CD11c$^+$) cells and M2-like (F4/80$^+$CD206$^+$) subsets were shown as mean ± SEM (n = 9–12 mice per genotype) and are representative of two independent experiments. *, $P < 0.05$; **, $P < 0.01$. (B) Total RNA isolated from M1- or M2-like macrophages was analyzed by quantitative real-time PCR and normalized to β-actin for the indicated genes. The mean value of each gene in M1-like cells from control groups was set to 1. Data are presented as mean ± SEM (n = 5–7 per genotype) and are representative of two independent experiments. (C) Total RNA was isolated from M1-like (F4/80$^+$CD11c$^+$) cells or M2-like (F4/80$^+$CD206$^+$) cells in aortic lesions and analyzed by quantitative real-time PCR and normalized to β-actin for the indicated genes. The mean value of each gene in M1-like cells from control groups was set to 1. Data are presented as mean ± SEM (n = 5–6 mice per genotype and are representative of two independent experiments. *, $P < 0.05$; **, $P < 0.01$.

significantly increased in MyD88-deficient M2- and M1-like macrophages compared with their corresponding control macrophages (Fig. 7 B). These data indicate that deletion of MyD88 in myeloid cells aborted HFD-induced switch of ATMs from M2- to M1-like subtype at cellular and molecular levels.

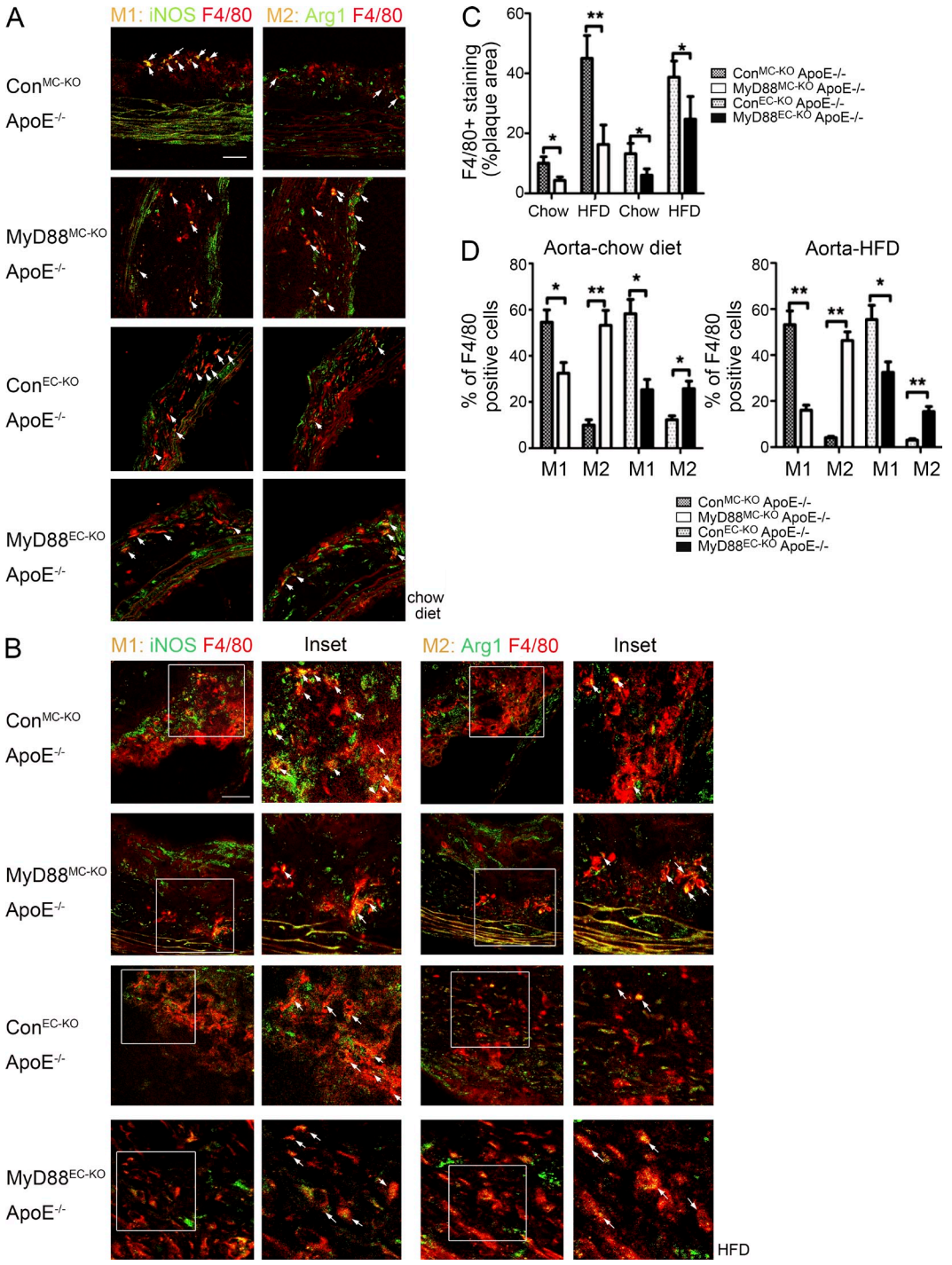

Figure 8. Deletion of MyD88 in myeloid cells and endothelial cells prevents M1 macrophage polarization in arterial tissue under hypercholesterolemia. Immunostaining of atherosclerotic lesions from MyD88$^{MC\text{-}KO}$ ApoE$^{-/-}$, MyD88$^{EC\text{-}KO}$ ApoE$^{-/-}$ female mice and their respective littermate controls on chow diet (A) or HFD (B) for 3 mo. Macrophages were identified as F4/80^{+} (red) cells. Co-expression of F4/80 and iNOS (green) or Arg1 (green) was identified by image overlay. (inset) Magnification of the zone delimited in the frame. Arrowheads indicate representative M1-like (F4/80^{+}iNOS^{+}) or M2-like (F4/80^{+}Arg1^{+}) cells. Bar, 20 µm. n = 4–5 mice per genotype. The results are representative of three independent experiments. (C) Lesional macrophage content as determined by percentage of F4/80^{+} staining area (mean ± SEM). (D) Enumeration of M1- or M2-like macrophages by immunofluorescence in aortic root sections as shown in G. Results are shown as mean ± SEM of five different sections per mouse and are representative of 4–5 mice per genotype with similar results. *, $P < 0.05$; **, $P < 0.01$.

Similar M1- and M2-associated gene expression patterns were observed in adipose tissues of mice bred onto ApoE$^{-/-}$ background fed on HFD (Fig. 6, E and F). It is interesting to note that MyD88 deficiency in myeloid cells also led to a shift from M1-associated [iNOS; TNF, IL-1, and IL-6] to M2-like [Arg1 and IL-10] gene expression in arterial tissue of chow- and HFD-fed mice (Fig. 5, A and C). This finding was confirmed by immunostaining of sections of aortic roots of MyD88$^{MC\text{-}KO}$ mice and littermate control mice on both chow diet and HFD (Fig. 8, A–D). MyD88 deficiency in myeloid cells indeed led to a shift from M1-like (F4/80$^+$iNOS$^+$) to M2-like (F4/80$^+$Arginase1$^+$) macrophages in the aortic lesions of mice on chow diet or HFD (Fig. 8, A–D). This result was further corroborated by gene expression profile from sorted macrophages from aortic tissues of HFD-fed mice. Inflammatory gene expression (iNOS and IL-6) was substantially reduced in sorted MyD88-deficient M1- (F4/80$^+$CD11c$^+$) and M2-like (F4/80$^+$CD206$^+$) macrophages compared with their corresponding control macrophages, respectively (Fig. 7 C). Importantly, M2-associated gene expression (Arg1 and IL-10) was much higher in M2-like than that in M1-like macrophages and significantly increased in MyD88-deficient M2- and M1-like macrophages compared with their wild-type control macrophages, respectively (Fig. 7 C).

Because myeloid-derived MyD88 had a dramatic impact on the ATM phenotype, we set up an adipocyte-macrophage ex vivo co-culture system to explore the cross-talk between adipocytes and macrophages. BMDMs and 3T3L1 adipocytes were cultured in the bottom and inner wells of Boyden chambers, respectively, which permitted passage of humoral factors between the chamber wells. Proinflammatory cytokine/chemokine mRNAs and proteins in the supernatant were higher in macrophages co-cultured with adipocytes than those in macrophages cultured alone (Fig. 9 A). The effects of co-culturing were augmented by the increase of ratios of adipocytes/macrophages (Fig. 9 A). Interestingly, we also found that Arginase-1 and CD206 (M2 markers) expression were reduced by co-culturing (Fig. 9 B). Furthermore, the expression of M1-associated genes, including IL-12a, IL-12b, IRF5, and NOS2 was concomitantly up-regulated by the increase of ratios of adipocytes/macrophages (Fig. 9 C). All these effects were reduced in MyD88KO BMDMs (Fig. 9, A–C), demonstrating that MyD88 participates in the cross-talk between adipocytes and macrophages, which might play a critical role in HFD-induced switching of ATMs from M2- to M1-like phenotype. The next question is what the relevant ligands here. ATMs are exposed to high local concentrations of FFAs

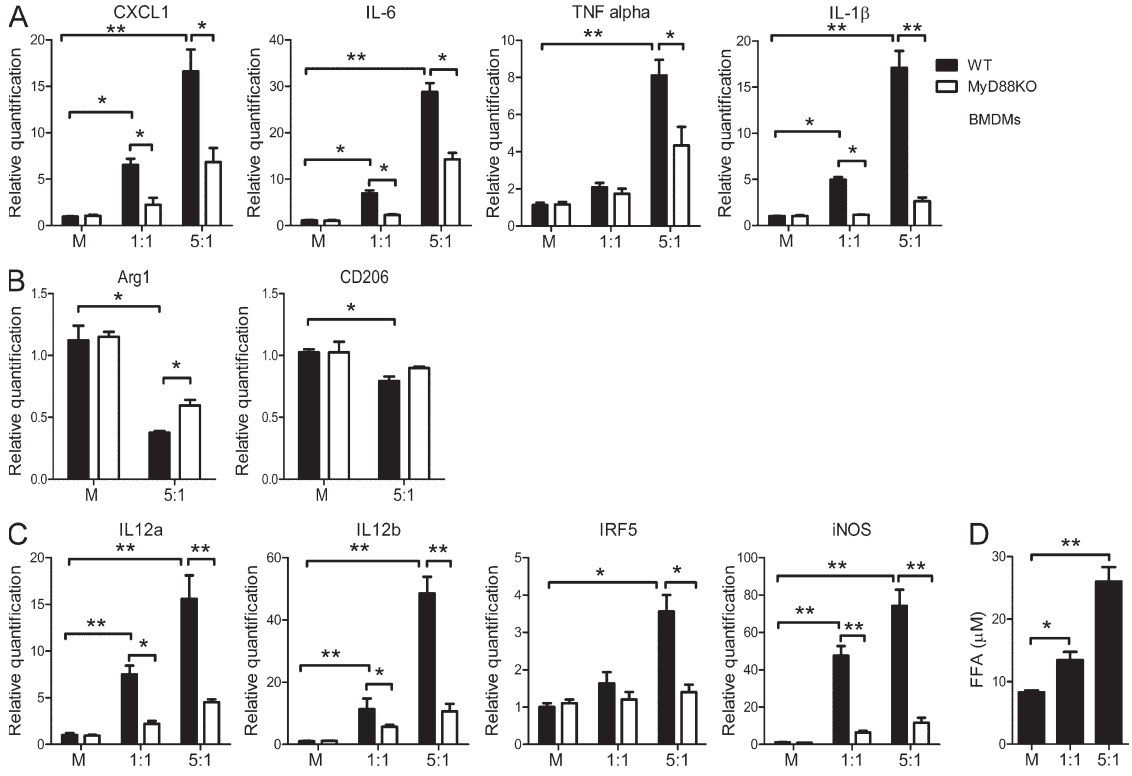

Figure 9. MyD88-dependent cross-talk between adipocytes and macrophages promotes M1 polarization. BMDMs of WT and MyD88KO male mice were plated in the bottom wells of Boyden chambers, with or without (indicated as M) 3T3 adipocytes in the inserts at a ratio of 1:1 or 5:1 (adipocytes, BMDM cell numbers). mRNA expression levels of (A) CXCL1, IL-6, TNF, IL-1β; (B) Arginase-1, CD206; (C) IL12a, IL12b, IRF5, and iNOS in the BMDMs were analyzed. The expression of mRNA normalized to β-actin expression. The data are presented as fold induction over the levels of mRNAs in WT macrophages cultured alone. $n = 5$ wells in each group. Data represent the mean ± SEM of the results from three independent experiments. (D) Concentration of FFA in the supernatant was measured by ELISA ($n = 5$ wells in each group). Data are expressed as mean ± SEM of the results from three independent experiments. *, $P < 0.05$; **, $P < 0.01$.

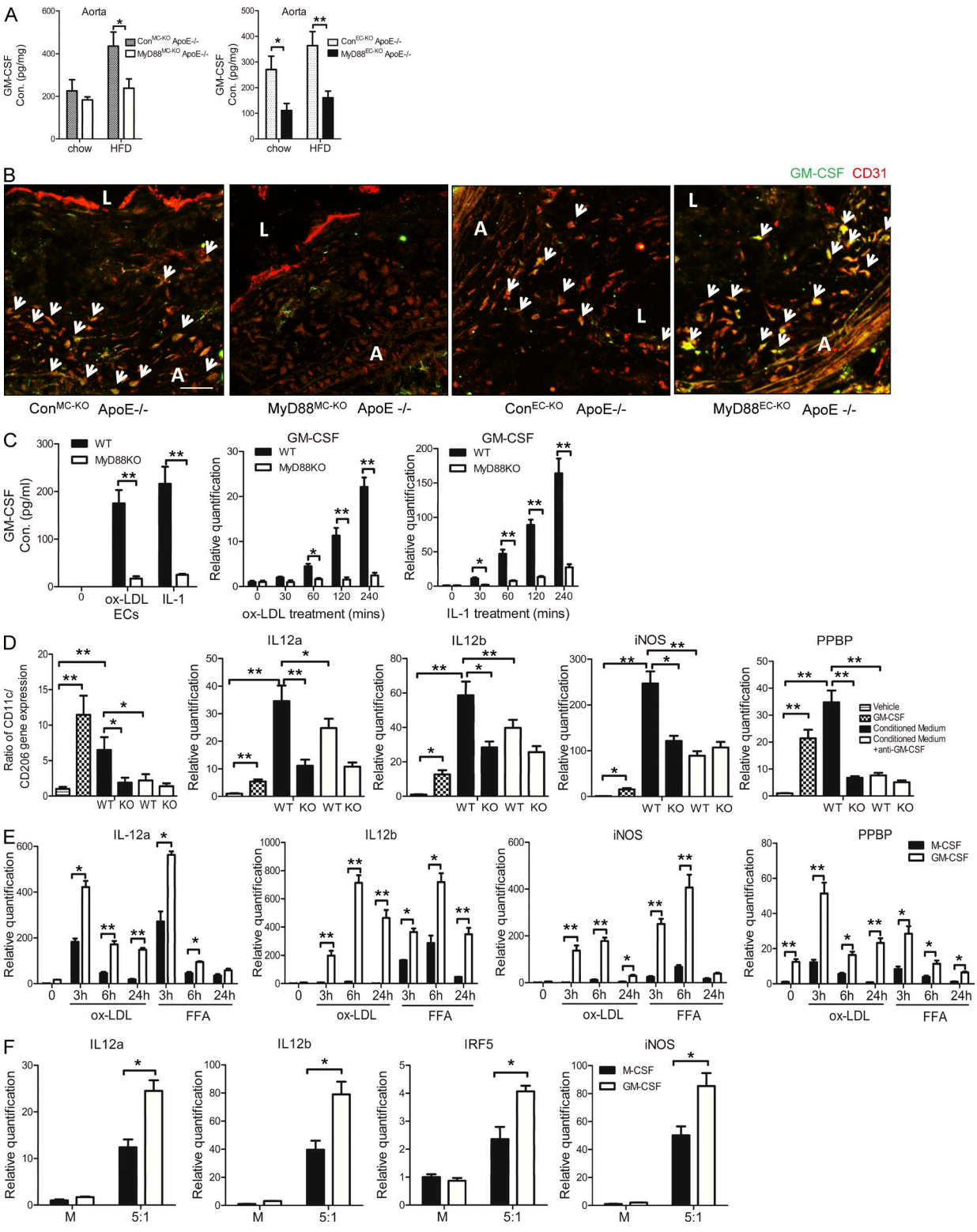

Figure 10. Endothelial MyD88 mediates GM-CSF production to prime M1 inflammatory macrophages. (A) Protein level of GM-CSF in whole aorta lysate taken from MyD88$^{MC\text{-}KO}$ ApoE$^{-/-}$, MyD88$^{EC\text{-}KO}$ ApoE$^{-/-}$ female mice and their respective littermate controls on chow diet or HFD for 12 wk beginning at 6 wk of age were analyzed by ELISA. Data are expressed as mean ± SEM (n = 5–6 per genotype) of the results from three independent experiments. *, $P < 0.05$; **, $P < 0.01$. (B) Immunostaining of GM-CSF (green) in conjunction with CD31 (red) were performed for frozen sections of aortic roots from MyD88$^{MC\text{-}KO}$ ApoE$^{-/-}$, MyD88$^{EC\text{-}KO}$ ApoE$^{-/-}$ female mice and their respective littermate controls on chow diet (3 mo of age). Then the tissues were examined by confocal microscopy. Arrowheads indicate representative CD31^{+} GM-CSF^{+} cells (bar, 20 µm; L, lumen; A, arterial wall). Shown are

released from enlarged adipocytes and augmented by increased lipolysis in obesity (Landin et al., 1990; Tsujita et al., 1995; Lafontan and Langin, 2009; Kosteli et al., 2010). We indeed detected FFA in the conditioned media of the co-culture experiment of adipocytes and macrophages by ELISA (Fig. 9 D). This finding suggests that FFA from adipocytes might serve as a TLR ligand to activate macrophages in our co-culture system. In support of this, we found that palmitate-induced inflammatory gene expression was substantially reduced in MyD88-deficient macrophages compared with that in control cells, while completely abolished in TLR4$^{-/-}$ and partially impaired in TLR2$^{-/-}$ macrophages, suggesting the possible role of saturated fatty acids (SFAs) in promoting TLR-MyD88–dependent switching of ATMs from M2- to M1-like inflammatory macrophages (unpublished data).

Endothelial MyD88 mediates GM-CSF production to prime M1-like inflammatory macrophages

Interestingly, MyD88$^{EC\text{-}KO}$ mice also showed moderate reduction in HFD-induced M1-like macrophages in adipose tissue (Fig. 6, C and D and Fig. 7, A and B). Endothelial-specific MyD88 deficiency consistently and substantially rescued insulin signaling in adipose tissue (Fig. 3, E and H). Furthermore, MyD88 deficiency in endothelial cells (MyD88$^{EC\text{-}KO}$ApoE$^{-/-}$) showed substantial reduction in lesion areas, aortic wall inflammation (including a shift from M1- to M2-like macrophages), and improved insulin sensitivity of aortas in both chow and HFD-fed mice (Fig. 4, B, D, and E; Fig. 5, B and D; Fig. 7 C; and Fig. 8, A–D). Based on these results, we hypothesized that MyD88 signaling in endothelial cells mediates the cross-talk with macrophages to impact on the initiation of atherosclerosis and diet-induced exacerbation on atherosclerotic lesions. Interestingly, we noticed that the expression of GM-CSF was substantially decreased in the arterial tissue and adipose tissue of MyD88$^{EC\text{-}KO}$ mice compared with controls (Fig. 5, B and D; Fig. 6 C; and Fig. 10 A). Immunostaining showed that GM-CSF was indeed colocalized with CD31^{+} endothelial cells in the aortic root lesions of Con$^{EC\text{-}KO}$ApoE$^{-/-}$ mice, which was abated in that of the MyD88$^{EC\text{-}KO}$ApoE$^{-/-}$ mice, demonstrating MyD88-dependent GM-CSF expression in endothelial cells (Fig. 10 B). GM-CSF is well-known for its function in promoting monocyte differentiation toward M1 proinflammatory macrophages (Verreck et al., 2004; Chitu and Stanley, 2006; Fleetwood et al., 2007; Hamilton, 2008; Kim et al., 2008; Waldo et al., 2008; Brochériou et al., 2011; Chinetti-Gbaguidi and Staels, 2011; Wolfs et al., 2011; Lacey et al., 2012). Based on our results and previous studies on GM-CSF, we proposed that MyD88-dependent signaling in endothelial cells induces the production of GM-CSF, which in turn primes the monocytes/macrophages to become M1-like inflammatory macrophages.

To test this hypothesis, we need to know the relevant ligands for the MyD88-dependent signaling in endothelial cells. Ox-LDL (oxidized and related modified forms of low density lipoproteins) is an endogenous TLR2/4 ligand, which accumulates in the vessel wall and is an emerging cardiovascular risk factor (Seimon et al., 2010; Su et al., 2011). ox-LDL may trigger TLR signaling in macrophages and directly on endothelial cells. In addition to ox-LDL, the endothelium, the interface between vascular structures and blood, can also be activated by a variety of circulating inflammatory stimuli (Aird, 2007), including TNF, IL-6, and IL-1. Therefore, the most relevant ligands for MyD88-dependent signaling in endothelial cells are ox-LDL and IL-1. Interestingly, we found that both ox-LDL and IL-1 can strongly induce GM-CSF expression in primary endothelial cells, which was completely abolished in MyD88-deficient endothelial cells (Fig. 10 C). We wondered then whether GM-CSF produced by ox-LDL– and IL-1–treated endothelial cells is able to influence the macrophage function. We found that the conditioned medium from ox-LDL–treated wild-type endothelial cells (but not MyD88-deficient endothelial cells) was able to induce GM-CSF-target gene PPBP (CXCL7; Brochériou et al., 2011; Chinetti-Gbaguidi and Staels, 2011) in CD11b^{+} monocytes and enhanced the expression of M1-associated genes including IL-12a, IL-12b, and iNOS (Fig. 10 D). Similar results were observed with IL-1–treated endothelial cells (unpublished data). Neutralization with anti–GM-CSF greatly reduced the expression of PPBP and M1-associated genes in monocytes in response to the conditioned medium from ox-LDL–treated endothelial cells (Fig. 10 D). Moreover, the conditioned medium from ox-LDL–treated

representative of five mice per genotype with similar results. (C) WT and MyD88-deficient (MyD88KO) primary aortic endothelial cells (ECs) were treated with ox-LDL (100 µg/ml) or IL-1 (1 ng/ml) for the indicated times (time 0 were treated with native LDL). Protein levels of GM-CSF in supernatant from cells treated for 24 h were analyzed by ELISA. The levels of GM-CSF mRNA were measured by real-time PCR and presented as fold induction over the expression of WT cells at time 0. (D) WT and MyD88 KO ECs were treated with ox-LDL for 24 h, and then changed into fresh medium. After 48 h, the medium was collected and used to culture sorted CD11b^{+} splenic monocytes for 24 h with or without anti–GM-CSF neutralizing antibody (conditioned medium, conditioned medium + anti–GM-CSF). Monocytes were cultured in normal medium as negative control (vehicle). Monocytes in normal medium were treated with 50 ng/ml recombinant GM-CSF alone as positive control (GM-CSF). Total RNA of monocytes was subjected to real-time PCR to measure the relative expression of CD11c, CD206, IL-12a, IL12b, iNOS, and PPBP. The fold induction was calculated as compared with vehicle group. (E) BD-derived cells were cultured in DMEM supplemented with 20% FBS and 20 ng/ml GM-CSF or 50 ng/ml M-CSF for 7 d, followed by treatment of ox-LDL and FFA (16:0; Palmitate, 5 µM) as indicated. Total RNA was subjected to real-time PCR to measure the expression of IL-12a, IL-12b, iNOS, and PPBP. The fold induction was calculated as compared with the cells primed by M-CSF at time 0. (F) BMDMs of WT male mice primed by either M-CSF or GM-CSF were plated in the bottom wells of Boyden chambers, with or without 3T3 adipocytes in the inserts at a ratio of 5:1 (adipocytes, BMDMs cell numbers). mRNA expression levels of IL12a, IL12b, IRF5, and iNOS in the BMDMs were analyzed. The fold induction was calculated as compared with the cells primed by M-CSF and cultured alone. mRNA expression was normalized to β-actin expression. (C–F) Data represent the mean ± SEM of triplicate samples from a single experiments, and all results are representative of three independent experiments. *, $P < 0.05$; **, $P < 0.01$.

wild-type endothelial cells (but not MyD88-deficient endothelial cells) was able to increase the ratio of CD11c (M1) to CD206 (M2), which was also blocked by anti–GM-CSF, supporting the role of GM-CSF in monocyte differentiation toward M1-like macrophages (Fig. 10 D). It is important to note that ox-LDL used in this study was generated by using MPO/H2O2/Nitrite system (see Materials and methods). We found that the ox-LDL generated by this protocol can consistently activate TLR-induced inflammatory genes and synergize with GM-CSF for up-regulation of M1-associated genes (Hazen et al., 1996; Hamilton et al., 1999; Hazen et al., 1999; Hazen and Heinecke, 1997; Febbraio et al., 2000; Podrez et al., 2000; Zhang et al., 2001; Baldus et al., 2003; Vita et al., 2004; Gallardo-Soler et al., 2008; van Tits et al., 2011).

Because ox-LDL has been shown to directly act on macrophages in vivo (Nagy et al., 1998; Fischer et al., 2002; Itabe et al., 2011; Rios et al., 2012), we wondered whether it is possible that GM-CSF produced by ox-LDL–activated endothelial cells synergizes with SFAs and ox-LDL to further promote M1-like proinflammatory macrophages. Palmitate and ox-LDL indeed enhanced the expression of M1-associated genes in GM-CSF–primed macrophages as compared with that in M-CSF–primed macrophages (Fig. 10 E). Interestingly, the expression of M1-associated gene expression was more robustly enhanced in the adipocyte–macrophage ex vivo co-culture system when using GM-CSF–primed macrophages as compared with that of M-CSF–primed macrophages (Fig. 10 F). Collectively, these results suggest a potential role of GM-CSF in priming ATMs to become M1-like macrophages during their cross-talk with adipocytes. It is important to note that endothelial-specific MyD88 deficiency substantially reduced HFD-induced GM-CSF expression in adipose tissue (Fig. 6 C), which was correlated with selective rescue of insulin signaling in adipose tissue of HFD-fed $MyD88^{EC\text{-}KO}$ mice (Fig. 3, E and H). These findings implicate the MyD88-dependent involvement of endothelial cells in the cross-talk between adipocytes and macrophages, which might be important for the initiation of obesity-associated inflammatory diseases. In support of this, endothelial MyD88 deficiency improved insulin sensitivity more dramatically at early phase (6 wk) compared to after 3 mo of HFD (Fig. 2, C and D); and $MyD88^{EC\text{-}KO}ApoE^{-/-}$ mice showed greater reduction in atherosclerotic lesions developed under chow diet (70% reduction) than under HFD (40% reduction).

DISCUSSION

The study presented here aimed to address how TLR signaling in different cellular compartments contributes to the initiation and pathogenesis of obesity-associated inflammatory diseases through the specific deletion of MyD88 in endothelial cells or myeloid cells. MyD88 deficiency in myeloid cells ameliorated diet-induced systemic inflammation and global insulin resistance, preserving insulin sensitivity in all the tested tissues including muscle, liver, and adipose tissue. On the other hand, endothelial-specific deficiency of MyD88 improved diet-induced insulin resistance at early phase with moderate effect on systemic inflammation, selectively restoring insulin sensitivity in adipose tissue. Whereas both myeloid- and endothelial-derived MyD88 were equally critical for the initiation of atherosclerosis in chow-fed ApoE-deficient mice, myeloid MyD88 clearly plays a more critical role than endothelial MyD88 in HFD-induced atherosclerosis. Collectively, these results for the first time demonstrate the nonredundant role of MyD88-dependent signaling in myeloid and endothelial cells for the development and progression of atherosclerosis and metabolic inflammatory diseases.

The participation of macrophages and endothelium in atherosclerosis has been extensively studied. In this study, we found that MyD88 deficiency in endothelial or myeloid cells inhibited vascular lesion formation in chow-fed ApoE-deficient mice, with similar reduction in atherosclerotic area (60–70%). It is interesting to note that MyD88-dependent pathology in chow-fed ApoE-deficient mice is restricted to the aorta, because under chow diet ApoE deficiency does not influence myeloid or endothelial MyD88-dependent WAT macrophage abundance, polarization, or inflammatory cytokine production. These results clearly indicate the critical role of the MyD88-dependent pathway in the interplay between the endothelium and macrophages in the aortic tissue during the initiation of atherosclerosis. The key initiating event in atherosclerosis is retention and oxidation of LDL in the vascular wall (Staels, 2002). Our study suggests that endothelial cell activation by ox-LDL through the TLR-MyD88-dependent pathway probably plays an important role in the initiation of atherosclerosis. Although ox-LDL strongly induces the expression of GM-CSF in a MyD88-dependent manner in endothelial cells, the expression of GM-CSF was greatly reduced in the arterial tissue of the chow-fed $MyD88^{EC\text{-}KO}ApoE^{-/-}$ mice compared with that in the control mice. GM-CSF was indeed detected in endothelial cells of atherosclerotic lesions, which was abolished in the $MyD88^{EC\text{-}KO}ApoE^{-/-}$ mice. Furthermore, ox-LDL–induced expression of M1-associated genes was more robust in GM-CSF-primed macrophages than that in M-CSF-primed macrophages. Therefore, MyD88-dependent GM-CSF production from endothelial cells might serve as an important link between endothelial cells and macrophages by promoting M1-like inflammatory macrophages. In support of this, GM-CSF has been shown to be important in plaque development. Using the hypercholesterolemic $ApoE^{-/-}$ mouse, it was found that GM-CSF treatment resulted in increased atherosclerotic lesion extent (Haghighat et al., 2007; Shaposhnik et al., 2007). LDLR-null mice have been used in a study that combined 5-bromo-2′-deoxyuridine pulse labeling with en face immunoconfocal microscopy to demonstrate that systemic injection of GM-CSF markedly increased intimal cell proliferation (including dendritic cells), whereas functional GM-CSF blockade inhibited proliferation(Zhu et al., 2009). Therefore, in addition to macrophage polarization, the impact of GM-CSF on dendritic cell proliferation may also contribute to the reduced lesions in our endothelial cell-MyD88–deficient mice. Future studies using cell type–specific GM-CSF receptor knockout mice

will be required to clarify the pathogenic role of GM-CSF in atherosclerosis.

Interestingly, when the mice were fed the HFD, there was a dramatic reduction (70%) in atherosclerotic area in MyD88^{MC-KO} ApoE$^{-/-}$ mice, but a more moderate reduction (40%) in MyD88^{EC-KO} ApoE$^{-/-}$ mice. The question is why myeloid MyD88 plays a more critical role than endothelial MyD88 in HFD-induced atherosclerosis. It is important to note that myeloid MyD88 deficiency led to greater improvement in HFD-induced systemic inflammation (circulating TNF, IL-6, and IL-1) and global insulin resistance than that by endothelial-specific MyD88 deficiency. Under HFD-induced systemic inflammation, in addition to ox-LDL, the endothelium can also be activated by a variety of circulating inflammatory stimuli (Aird, 2007), including TNF and IL-6. As a result, the activation of endothelium, the interface between vascular structures and blood, becomes less dependent on the MyD88-dependent pathway over the course of HFD. Consistently, endothelial MyD88 deficiency improved global insulin resistance more dramatically at early phase (6 wk after HFD) than that after 3 mo of HFD.

One important question is how systemic inflammation is initiated in a HFD setting. Previous studies have suggested that metabolically triggered inflammation in white adipose tissue plays a key role in the initiation of metabolic syndrome (Hotamisligil et al., 1993; Neels and Olefsky, 2006; Nishimura et al., 2009; Wajchenberg et al., 2009). ATMs are exposed to high local concentrations of FFAs released from adipocytes in obesity, and these serve as important activating ligands for TLR4 and TLR2 signaling in macrophages (Tsujita et al., 1995; Suganami et al., 2005, 2007; Nguyen et al., 2007; Miyazaki et al., 2011; Prieur et al., 2011). The results from our co-culture model suggest that MyD88 participates in the cross-talk between adipocytes and macrophages and FFA released by adipocytes might be one of the initial ligands for TLR-MyD88 in this cross-talk. The cytokines (e.g., IL-1 and IL-6) may feedback on adipocytes to further promote this cross-talk (Rotter et al., 2003; Trujillo et al., 2004; Lagathu et al., 2006; Jager et al., 2007; Stienstra et al., 2010). Compared with controls, MyD88^{MC-KO} mice consistently showed markedly reduced infiltration of macrophages and decreased adipose expression of inflammatory genes. Furthermore, the elimination of MyD88 in myeloid cells increased the number of M2-like macrophages (CD11c^{-}CD206^{+}), with decreased M1-like macrophages (CD11c^{+}CD206^{-}) in the adipose tissue, confirming the critical role of MyD88-dependent signaling in HFD-induced ATM switching from M2- to M1-like macrophages. Myeloid-specific MyD88-dependent switch of ATMs from M2-like to M1-like might play a key role in the initiation of obesity-associated inflammatory diseases. However, it is important to note that in addition to adipose tissue, myeloid-specific MyD88 deficiency also preserved insulin sensitivity in liver and muscle, which probably contributes to the improvement of HFD-induced global insulin resistance and systemic inflammation. Because CD11bCre mediates deletion of floxed sequences in myeloid cells, we crossed MyD88$^{fl/fl}$ mice with LysMCre mice to delete MyD88 in macrophages. Preliminary data from LysMCreMyD88$^{fl/fl}$ mice showed similar results with that in MyD88^{MC-KO} mice as compared with the littermate controls (unpublished data).

Interestingly, MyD88^{EC-KO} mice also showed moderate reduction in macrophage infiltration, M2- to M1-like switching, and adipose expression of those proinflammatory cytokine and chemokine genes. Whereas FFAs released from adipocytes might directly act on endothelial cells, IL-1 released from FFA-induced M1-like macrophages could also activate endothelium through a paracrine manner. Although IL-1 strongly induced the expression of GM-CSF, the GM-CSF levels were substantially reduced in adipose tissue of HFD-fed MyD88^{EC-KO} mice. IL-1–induced GM-CSF in endothelial cells was able to promote M1-like inflammatory macrophages. Furthermore, the expression of M1-associated gene expression was more robustly enhanced in the adipocyte-macrophage ex vivo co-culture system when using GM-CSF–primed macrophages as compared with that of M-CSF–primed macrophages. Thus, endothelial MyD88 might impact on switching of ATMs from M2- to M1-like through the production of GM-CSF, which may account for the selective rescue of insulin sensitivity in adipose tissue of HFD-fed MyD88^{EC-KO} mice. In support of this, endothelial deletion of MyD88 also moderately reduced M1-like macrophages in the aortas, with substantial reduction of GM-CSF expression, which correlated with improved insulin sensitivity of aortic tissues from HFD-fed MyD88^{EC-KO} mice. It is important to mention that the GM-CSF levels were not significantly reduced in liver and muscle of HFD-fed MyD88^{EC-KO} mice (unpublished data), which might explain why these two tissues remain insulin insensitive in HFD-fed MyD88^{EC-KO} mice.

It is important to note that in addition to MyD88, TLR4 also utilizes TRIF to mediate NF-κB activation to up-regulate inflammatory gene expression. TRIF deficiency (Lundberg et al., 2013) or *TRIF*^{LPS2} lack-of-function mutation were shown to be atheroprotective in hyperlipidemic LDL receptor knockout (LDLr$^{-/-}$) mice (Richards et al., 2013). Both studies supported a critical role of TRIF-dependent pathway in the pathogenesis of atherosclerosis. However, it is important to point out that TLR4 specifically utilizes TRIF to mediate the activation of transcription factor IRF3 to up-regulate type 1 IFN production, which in turn impacts on IL-10 production (Petrasek et al., 2011). Furthermore, it was reported that TRIF is not required for TLR4 signaling in endothelial cells (Harari et al., 2006), which was confirmed by our own studies in primary aortic vascular endothelial cells (unpublished data). Therefore, mice with cell type–specific TRIF deletion will be critical reagents for future studies to compare the molecular and cellular mechanisms by which MyD88- versus TRIF-dependent pathway contributes to the development and pathogenesis obesity-associated inflammatory diseases.

In summary, this study has demonstrated that MyD88-dependent signaling in both myeloid and endothelial cells contributed to the initiation/progression of atherosclerosis and the development and pathogenesis of HFD-induced inflammatory

diseases. Both myeloid- and endothelial-derived MyD88 are critical for the initiation of atherosclerosis in chow-fed mice. One possible mechanism is that ox-LDL activates endothelial cells to produce GM-CSF, which in turn primes the monocytes in the arterial tissues and synergizes with ox-LDL to promote M1 inflammatory macrophages. On the other hand, MyD88-dependent signaling in myeloid cells makes a greater contribution to the development of HFD-induced systemic inflammation and consequent exacerbation on atherosclerosis. FFAs released from adipocytes act on ATMs to promote HFD-induced switching of ATMs from M2-like to M1-like, resulting in systemic inflammation and aggravating atherosclerotic lesions. Nevertheless, endothelial-derived MyD88 still has a noticeable contribution to the diet-induced inflammatory diseases, possibly also through the production of GM-CSF to feedback on macrophages. Future studies are required to elucidate how the cell type–specific, MyD88-mediated signaling events contribute to the cross-talks among adipocytes, macrophages, and endothelial cells to establish the diet-induced inflammatory state, leading to inflammatory diseases associated with metabolic syndrome.

MATERIALS AND METHODS

Animals. CD11bCre transgenic mice were provided by G. Kollias (Biomedical Sciences Research Centre "Alexander Fleming," Vari, Greece; Boillée et al., 2006). Tie2eCre transgenic mice were a gift of X.-Y. Fu (National University of Singapore, Singapore; Kano et al., 2003). MyD88 flox mice were provided by A. DeFranco (University of California, San Francisco, CA; Hou et al., 2008). All these transgenic mice used backcrossed 10 times to C57/BL6 background. ApoE$^{-/-}$ mice in the C57/BL6 background were purchased from The Jackson Laboratory. Mice were housed in a specific pathogen–free facility (12-h light/dark cycle) and were fed either standard rodent chow or a Western style HFD (Harlan Teklad 88137; Tordjman et al., 2001; Chen et al., 2005; Alkhouri et al., 2010; Fernández-Real et al., 2011). Animals were fasted overnight and blood samples were taken for assessment of insulin (Crystal Chem), FFA(Cayman), cholesterol (Sigma-Aldrich), triglycerides (Sigma-Aldrich) and IL-1β, IL-6, TNF, CXCL1 (R&D Systems) levels according to manufacturer's instructions. All experimental procedures were performed with the approval of the Institutional Animal Care and Use Committee of Cleveland Clinic (Cleveland, OH).

Primary cell isolation. BM-derived macrophages (BMDMs) were differentiated from BD flushed from the tibia and femur of mice using DMEM. The cells were cultured in DMEM supplemented with 20% FBS and 30% L929 supernatant for 5 d. Mouse aortic endothelial cells (MAVECs) were harvested from mouse aorta under sterile conditions as previously described (Hatley et al., 2003). The aorta was excised; all periadventitial fat was removed, and the aortic pieces were placed onto Matrigel in DMEM plus 15% heat-inactivated FBS following the methods outlined by Shi et al. (2000). After 3 d, the aortic explants were removed, and the endothelial cells were allowed to grow in DMEM plus 15% heat-inactivated FBS supplemented with 180 µg/ml heparin and 20 µg/ml endothelial cell growth supplement. At confluence, the cells were passaged using dispase, and then cultured for 2 d in DMEM plus 15% heat-inactivated FBS containing D-valine to eliminate possible fibroblast contamination. After 2 d, the EC were returned to growth medium without D-valine and allowed to grow to confluence. Mouse endothelial cell cultures were used in experiments from passages 2–4. Spleens were minced and digested with Liberase Blendzyme 2 for 15 min in PBS at 21°C, passed through a 40-mm cell strainer, treated with ACK Buffer (Lonza) to remove red cells, and resuspended in PBE (PBS with 0.5% BSA, endotoxin free; 1 mM EDTA). Splenocytes were subsequently sorted on a Dako MoFlo. Postsort analysis confirmed purity of 96% and viability of 95%.

Biological reagents and cell culture. Human low-density lipoprotein (LDL, 1.019 < density < 1.063) was isolated from plasma of normolipidemic donors by sequential ultracentrifugation. Native and modified LDL preparations were tested for possible endotoxin contamination using a Limulus amebocyte lysate kit (Cambrex). ox-LDL was prepared by incubating LDL (0.2 mg protein/ml) at 37°C in 50 mM sodium phosphate, pH 7.0, 100 mM DTPA (diethylene-triamine-pentaacetic acid) in the presence of 30 nM myeloperoxidase, 100 mg/ml glucose, 20 ng/ml glucose oxidase (grade II; Boehringer Mannheim Biochemicals), and 0.5 mM $NaNO_2$ for 8 h unless otherwise specified. Preliminary studies demonstrated that under these conditions, a constant flux of H_2O_2 (0.18 mM/min) is generated by the glucose oxidase system. Unless otherwise stated, oxidation reactions were terminated by addition of 40 mM butylated hydroxytoluene (100 mM ethanolic stock) and 300 nM catalase to the reaction mixture (Abu-Soud and Hazen, 2000a,b). FFA solutions were prepared as described previously (Karaskov et al., 2006). In brief, 100-mM palmitate (Sigma-Aldrich) stocks were prepared in 0.1 M NaOH at 70°C and filtered. 5% (wt/vol) FFA-free BSA (Sigma-Aldrich) solution was prepared in double-distilled H_2O and filtered. A 5-mM FFA/5% BSA solution was prepared by complexing an appropriate amount of FFA to 5% BSA in a 60°C water bath. The aforementioned solution was then cooled to room temperature and diluted 1:5 in RPMI 1640 without FBS to a final concentration of 1 mM FFA/1% BSA. Antibodies against MyD88, β-actin, and phosphotyrosine (PY20) were purchased from Santa Cruz Biotechnology. Antibodies against p85-PI3K, GM-CSF, M-CSF and AKT were purchased from Abcam. Anti-Insulin receptor substrate 1 (IRS1) antibody was purchased from Upstate Biotechnology. Anti-phospho-Akt (Ser473) antibody, anti-arginase 1, and anti-iNOS were purchased from Cell Signaling Technology. Anti-F4/80 was purchase from Ab Serotec. 3T3 L1 preadipocytes were cultured in DMEM, 10% FBS, and 1% penicillin/streptomycin, and differentiated using the adipogenesis kit at 37°C and 5% CO_2 (Cayman Chemical). Differentiation was initiated 1 d after 100% confluence was reached. Confluent 3T3-L1 cells preadipocytes were treated with 50 ml initiation medium containing 500 µM IBMX, 10 µM dexamethasone, 10 µg/ml insulin in DMEM/10% FBS for 2 d. Afterward, medium was changed to 40 ml progression medium consisting of DMEM/10% FBS supplemented with 10 µg/ml insulin. The 3T3-L1 cells were incubated with progression medium for 2 d. Subsequently, medium was changed at day 6 into 50 ml fresh DMEM/10% FBS, followed by another 2 d incubation at 37°C. 8 d after the initiation of differentiation, 3T3-L1 cells were ready for co-culture experiments. Preadipocytes were only differentiated and used before passage 12, and >95% of cells displayed the fully differentiated phenotype. For the co-culture system, differentiated 3T3-L1 adipocytes were co-cultured with differentiated BMDMs in DMEM/10% FBS for a maximum of 24 h using 6-well plates containing Transwell inserts with a 0.4 m^2 porous membrane (Falcon). 1×10^4 BMDMs were seeded on the bottom of the well, whereas 1×10^4 or 5×10^4 3T3-L1 adipocytes were seeded with into the insert. BMDMs cultured in the well without adipocytes seeded were set as control culture. After 24 h of incubation, supernatants were collected and centrifuged for 10 min at 10,000 *g* and 4°C; samples were stored at −20°C for cytokines measurement. mRNA was collected from BMDMs for further gene expression analysis.

GTT/Insulin tolerance test (ITT). GTTs were performed by i.p. injection of 2 g/kg body weight of dextrose (Abbott Laboratories) after overnight fast. For ITTs, mice were injected with insulin (1 mU/g BW; Sigma-Aldrich) i.p. after 3-h fasting. Blood samples were obtained at 0, 15, 30, 60, 90, and 120 min time points and glucose levels were measured with an ultra-one glucometer.

Insulin signaling analysis. Epididymal fat, liver, and quadriceps muscle were collected from mice in the basal state or 5 min after an i.p. injection of insulin (25 mU/kg), and quickly frozen in liquid nitrogen. Frozen tissues were homogenized on ice in a Triton-containing lysis buffer (0.5% Triton X-100, 20 mM Hepes, pH 7.4, 150 mM NaCl, 12.5 mM β-glycerophosphate,

1.5 mM $MgCl_2$, 10 mM NaF, 2 mM dithiothreitol (DTT), 1 mM sodium orthovanadate, 2 mM EGTA, 1 mM phenylmethylsulfonyl fluoride and complete protease inhibitor cocktail from Roche), and then ground and rocked for 1 h in the cold room. Cellular debris was removed by centrifugation at 10,000 *g* for 5 min. Immunoprecipitations were performed with the indicated amount of lysates. Supernatants were incubated with 5 µg of polyclonal antibody overnight and then incubated with protein A beads for another 1 h at 4°C. Samples were washed extensively with lysis buffer before solubilization in SDS sample buffer. Bound proteins and whole lysates (40 µg) were resolved by 4–12% or 4–20% SDS-PAGE and transferred to nitrocellulose membranes (Bio-Rad Laboratories). Individual proteins were detected with the specific antibodies and visualized on film using horseradish peroxidase–conjugated secondary antibodies (Bio-Rad Laboratories) and Western Lightning Enhanced Chemiluminescence (Perkin Elmer Life Sciences). The levels of IRS1, p85-PI3K, activated AKT (pSer473, pAKT), and total AKT, were determined by immunoblotting of the whole lysates. Protein extracts were immunoprecipitated with anti–IRS-1, followed by Western analyses with antibodies specific for phosphotyrosine (PY20, pY) or p85-PI3K.

Atherosclerosis lesion measurements. Atherosclerotic lesions were quantified by two independent and blinded assessments (Febbraio et al., 2004). Mice were sacrificed by pentobarbital overdose, perfused with PBS and 10% formalin (Formalde-Fresh; Thermo Fisher Scientific), and the entire aortic tree, including the heart, dissected free of fat and other tissue. Aortae were stained with oil red O, and digitally scanned. En face lesion area was assessed using Adobe Photoshop software, analyzed by Mann-Whitney *U* test. Data are expressed as percent of total aortic area ± SEM.

Immunohistochemistry. Freshly isolated adipose tissues were fixed with phosphate-buffered formalin overnight, and then paraffin wax embedded and subsequently deparaffinized. 5-µm sections were incubated overnight with monoclonal anti-F4/80 antibody (AbD Serotec). After washing in PBS, slides were stained and developed using ABC staining system (Santa Cruz Biotechnology) and counterstained with hematoxylin (Sigma-Aldrich). The total number of cells and crown-like structure were counted in 10 different high-power fields from each section. Frozen aortic root sections were blocked with 2% BSA (diluted in PBS) containing 0.1% sodium azide for 1 h, followed by overnight incubation with the primary antibody (1:50 dilution for anti–GM-CSF, and 1:100 for anti-CD31; or 1:50 for anti-F4/80, 1:100 for anti-Arginase1, and 1:100 for anti-iNOS) at 4°C. After washing in PBS, slides were incubated with the fluorochrome-conjugated secondary antibody (Alexa Fluor 488–labeled donkey anti–rat IgG and Alexa Fluor 594–labeled mouse anti–rabbit IgG, or Alexa Fluor 488–labeled mouse anti–rabbit IgG and Alexa Fluor 594 labeled donkey anti–rat IgG 1:200 diluted in blocking buffer) for 2 h in the dark at room temperature, washed again in PBS and mounted with VECTASHIELD containing anti-fade reagent (Vector Laboratories, Inc.). Fluorescent images were acquired using a Leica confocal microscope. No specific immunostaining was seen in sections incubated with PBS rather than the primary antibody.

Flow cytometry. The visceral adipose tissue (epididymal fat pad) and aorta were digested as described previously (Galkina et al., 2006; Lumeng et al., 2007). SVF cells from adipose depots and aortic single cells were stained with anti-F4/80, CD11b, CD206, and CD11c (eBioscience) to identify macrophage subsets. FACS analysis was conducted using FACSCalibur (BD) and the FACS data were analyzed by after collection compensation using FlowJo (Tree Star) software.

Quantitative real-time PCR. Total RNA was prepared from endothelial cells or BMDMs of mice with TRIzol reagent (Invitrogen). Tissues were preserved in RNAlater solution (Ambion), and subsequently homogenized in TRIzol reagent. Three micrograms of total RNA were then used for the reverse transcription reaction using SuperScript reverse transcription (Invitrogen). Quantitative PCR was performed using an AB 7300 Real-Time PCR System, and gene expression was examined by SYBR GREEN PCR Master Mix (Applied Biosystems). PCR amplification was performed in triplicate, and water was used to replace cDNA in each run as a negative control. The reaction protocol included preincubation at 95°C to activate FastStart DNA polymerase for 10 min, 40 cycles of amplification beginning with 15 s of denaturation at 95°C, followed by annealing/extension for 60 s at 60°C. The results were normalized to the housekeeping gene mouse β-actin. Primer sequences were designed using online tools from GeneScript. The primer sequences used will be distributed upon request.

Statistical analysis. Data are expressed as mean ± SEM. Differences were analyzed by Student *t* test and one-way ANOVA. $P \leq 0.05$ was considered significant.

This work was supported by grants from National Institutes of Health (2PO1 HL 029582-26A1; 2PO1CA062220-16A1).

The authors have no conflicting financial interests.

Submitted: 24 June 2013
Accepted: 20 February 2014

REFERENCES

Abu-Soud, H.M., and S.L. Hazen. 2000a. Nitric oxide is a physiological substrate for mammalian peroxidases. *J. Biol. Chem.* 275:37524–37532. http://dx.doi.org/10.1074/jbc.275.48.37524

Abu-Soud, H.M., and S.L. Hazen. 2000b. Nitric oxide modulates the catalytic activity of myeloperoxidase. *J. Biol. Chem.* 275:5425–5430. http://dx.doi.org/10.1074/jbc.275.8.5425

Aird, W.C. 2007. Phenotypic heterogeneity of the endothelium: I. Structure, function, and mechanisms. *Circ. Res.* 100:158–173. http://dx.doi.org/10.1161/01.RES.0000255691.76142.4a

Alkhouri, N., A. Gornicka, M.P. Berk, S. Thapaliya, L.J. Dixon, S. Kashyap, P.R. Schauer, and A.E. Feldstein. 2010. Adipocyte apoptosis, a link between obesity, insulin resistance, and hepatic steatosis. *J. Biol. Chem.* 285:3428–3438. http://dx.doi.org/10.1074/jbc.M109.074252

Avouac, J., and Y. Allanore. 2008. Cardiovascular risk in rheumatoid arthritis: effects of anti-TNF drugs. *Expert Opin. Pharmacother.* 9:1121–1128. http://dx.doi.org/10.1517/14656566.9.7.1121

Baldus, S., C. Heeschen, T. Meinertz, A.M. Zeiher, J.P. Eiserich, T. Münzel, M.L. Simoons, C.W. Hamm, and C. Investigators; CAPTURE Investigators. 2003. Myeloperoxidase serum levels predict risk in patients with acute coronary syndromes. *Circulation.* 108:1440–1445. http://dx.doi.org/10.1161/01.CIR.0000090690.67322.51

Björkbacka, H., V.V. Kunjathoor, K.J. Moore, S. Koehn, C.M. Ordija, M.A. Lee, T. Means, K. Halmen, A.D. Luster, D.T. Golenbock, and M.W. Freeman. 2004. Reduced atherosclerosis in MyD88-null mice links elevated serum cholesterol levels to activation of innate immunity signaling pathways. *Nat. Med.* 10:416–421. http://dx.doi.org/10.1038/nm1008

Boillée, S., K. Yamanaka, C.S. Lobsiger, N.G. Copeland, N.A. Jenkins, G. Kassiotis, G. Kollias, and D.W. Cleveland. 2006. Onset and progression in inherited ALS determined by motor neurons and microglia. *Science.* 312:1389–1392. http://dx.doi.org/10.1126/science.1123511

Brochériou, I., S. Maouche, H. Durand, V. Braunersreuther, G. Le Naour, A. Gratchev, F. Koskas, F. Mach, J. Kzhyshkowska, and E. Ninio. 2011. Antagonistic regulation of macrophage phenotype by M-CSF and GM-CSF: implication in atherosclerosis. *Atherosclerosis.* 214:316–324. http://dx.doi.org/10.1016/j.atherosclerosis.2010.11.023

Brown, J., H. Wang, G.N. Hajishengallis, and M. Martin. 2011. TLR-signaling networks: an integration of adaptor molecules, kinases, and cross-talk. *J. Dent. Res.* 90:417–427. http://dx.doi.org/10.1177/0022034510381264

Caligiuri, G., A. Nicoletti, X. Zhou, I. Törnberg, and G.K. Hansson. 1999. Effects of sex and age on atherosclerosis and autoimmunity in apoE-deficient mice. *Atherosclerosis.* 145:301–308. http://dx.doi.org/10.1016/S0021-9150(99)00081-7

Cani, P.D., J. Amar, M.A. Iglesias, M. Poggi, C. Knauf, D. Bastelica, A.M. Neyrinck, F. Fava, K.M. Tuohy, C. Chabo, et al. 2007. Metabolic endotoxemia initiates obesity and insulin resistance. *Diabetes.* 56:1761–1772. http://dx.doi.org/10.2337/db06-1491

Cani, P.D., R. Bibiloni, C. Knauf, A. Waget, A.M. Neyrinck, N.M. Delzenne, and R. Burcelin. 2008. Changes in gut microbiota control metabolic endotoxemia-induced inflammation in high-fat diet-induced obesity and diabetes in mice. *Diabetes*. 57:1470–1481. http://dx.doi.org/10.2337/db07-1403

Chen, N., L. Liu, Y. Zhang, H.N. Ginsberg, and Y.H. Yu. 2005. Whole-body insulin resistance in the absence of obesity in FVB mice with overexpression of Dgat1 in adipose tissue. *Diabetes*. 54:3379–3386. http://dx.doi.org/10.2337/diabetes.54.12.3379

Cheung, A.T., J. Wang, D. Ree, J.K. Kolls, and M. Bryer-Ash. 2000. Tumor necrosis factor-alpha induces hepatic insulin resistance in obese Zucker (fa/fa) rats via interaction of leukocyte antigen-related tyrosine phosphatase with focal adhesion kinase. *Diabetes*. 49:810–819. http://dx.doi.org/10.2337/diabetes.49.5.810

Chi, H., E. Messas, R.A. Levine, D.T. Graves, and S. Amar. 2004. Interleukin-1 receptor signaling mediates atherosclerosis associated with bacterial exposure and/or a high-fat diet in a murine apolipoprotein E heterozygote model: pharmacotherapeutic implications. *Circulation*. 110:1678–1685. http://dx.doi.org/10.1161/01.CIR.0000142085.39015.31

Chinetti-Gbaguidi, G., and B. Staels. 2011. Macrophage polarization in metabolic disorders: functions and regulation. *Curr. Opin. Lipidol.* 22:365–372. http://dx.doi.org/10.1097/MOL.0b013e32834a77b4

Chitu, V., and E.R. Stanley. 2006. Colony-stimulating factor-1 in immunity and inflammation. *Curr. Opin. Immunol.* 18:39–48. http://dx.doi.org/10.1016/j.coi.2005.11.006

Creely, S.J., P.G. McTernan, C.M. Kusminski, M. Fisher, N.F. Da Silva, M. Khanolkar, M. Evans, A.L. Harte, and S. Kumar. 2007. Lipopolysaccharide activates an innate immune system response in human adipose tissue in obesity and type 2 diabetes. *Am. J. Physiol. Endocrinol. Metab.* 292:E740–E747. http://dx.doi.org/10.1152/ajpendo.00302.2006

Dasu, M.R., S. Ramirez, and R.R. Isseroff. 2012. Toll-like receptors and diabetes: a therapeutic perspective. *Clin. Sci.* 122:203–214. http://dx.doi.org/10.1042/CS20110357

De Taeye, B.M., T. Novitskaya, O.P. McGuinness, L. Gleaves, M. Medda, J.W. Covington, and D.E. Vaughan. 2007. Macrophage TNF-alpha contributes to insulin resistance and hepatic steatosis in diet-induced obesity. *Am. J. Physiol. Endocrinol. Metab.* 293:E713–E725. http://dx.doi.org/10.1152/ajpendo.00194.2007

Dixon, W.G., and D.P. Symmons. 2007. What effects might anti-TNFalpha treatment be expected to have on cardiovascular morbidity and mortality in rheumatoid arthritis? A review of the role of TNFalpha in cardiovascular pathophysiology. *Ann. Rheum. Dis.* 66:1132–1136. http://dx.doi.org/10.1136/ard.2006.063867

Ehses, J.A., G. Lacraz, M.H. Giroix, F. Schmidlin, J. Coulaud, N. Kassis, J.C. Irminger, M. Kergoat, B. Portha, F. Homo-Delarche, and M.Y. Donath. 2009. IL-1 antagonism reduces hyperglycemia and tissue inflammation in the type 2 diabetic GK rat. *Proc. Natl. Acad. Sci. USA*. 106:13998–14003. http://dx.doi.org/10.1073/pnas.0810087106

Elhage, R., A. Maret, M.T. Pieraggi, J.C. Thiers, J.F. Arnal, and F. Bayard. 1998. Differential effects of interleukin-1 receptor antagonist and tumor necrosis factor binding protein on fatty-streak formation in apolipoprotein E-deficient mice. *Circulation*. 97:242–244. http://dx.doi.org/10.1161/01.CIR.97.3.242

Emanuela, F., M. Grazia, R. Marco, L. Maria Paola, F. Giorgio, and B. Marco. 2012. Inflammation as a Link between Obesity and Metabolic Syndrome. *J. Nutr. Metab.* 2012:476380. http://dx.doi.org/10.1155/2012/476380

Erridge, C. 2011. Diet, commensals and the intestine as sources of pathogen-associated molecular patterns in atherosclerosis, type 2 diabetes and non-alcoholic fatty liver disease. *Atherosclerosis*. 216:1–6. http://dx.doi.org/10.1016/j.atherosclerosis.2011.02.043

Febbraio, M., E.A. Podrez, J.D. Smith, D.P. Hajjar, S.L. Hazen, H.F. Hoff, K. Sharma, and R.L. Silverstein. 2000. Targeted disruption of the class B scavenger receptor CD36 protects against atherosclerotic lesion development in mice. *J. Clin. Invest.* 105:1049–1056. http://dx.doi.org/10.1172/JCI9259

Febbraio, M., E. Guy, and R.L. Silverstein. 2004. Stem cell transplantation reveals that absence of macrophage CD36 is protective against atherosclerosis. *Arterioscler. Thromb. Vasc. Biol.* 24:2333–2338. http://dx.doi.org/10.1161/01.ATV.0000148007.06370.68

Fernández-Real, J.M., S. Pérez del Pulgar, E. Luche, J.M. Moreno-Navarrete, A. Waget, M. Serino, E. Sorianello, A. Sánchez-Pla, F.C. Pontaque, J. Vendrell, et al. 2011. CD14 modulates inflammation-driven insulin resistance. *Diabetes*. 60:2179–2186. http://dx.doi.org/10.2337/db10-1210

Ferrante, A., A.R. Giardina, F. Ciccia, G. Parrinello, G. Licata, G. Avellone, E. Giardina, R. Impastato, and G. Triolo. 2009. Long-term anti-tumour necrosis factor therapy reverses the progression of carotid intima-media thickness in female patients with active rheumatoid arthritis. *Rheumatol. Int.* 30:193–198. http://dx.doi.org/10.1007/s00296-009-0935-2

Fischer, B., A. von Knethen, and B. Brüne. 2002. Dualism of oxidized lipoproteins in provoking and attenuating the oxidative burst in macrophages: role of peroxisome proliferator-activated receptor-gamma. *J. Immunol.* 168:2828–2834.

Fleetwood, A.J., T. Lawrence, J.A. Hamilton, and A.D. Cook. 2007. Granulocyte-macrophage colony-stimulating factor (CSF) and macrophage CSF-dependent macrophage phenotypes display differences in cytokine profiles and transcription factor activities: implications for CSF blockade in inflammation. *J. Immunol.* 178:5245–5252.

Fraczek, J., T.W. Kim, H. Xiao, J. Yao, Q. Wen, Y. Li, J.L. Casanova, J. Pryjma, and X. Li. 2008. The kinase activity of IL-1 receptor-associated kinase 4 is required for interleukin-1 receptor/toll-like receptor-induced TAK1-dependent NFkappaB activation. *J. Biol. Chem.* 283:31697–31705. http://dx.doi.org/10.1074/jbc.M804779200

Fresno, M., R. Alvarez, and N. Cuesta. 2011. Toll-like receptors, inflammation, metabolism and obesity. *Arch. Physiol. Biochem.* 117:151–164. http://dx.doi.org/10.3109/13813455.2011.562514

Fujisaka, S., I. Usui, A. Bukhari, M. Ikutani, T. Oya, Y. Kanatani, K. Tsuneyama, Y. Nagai, K. Takatsu, M. Urakaze, et al. 2009. Regulatory mechanisms for adipose tissue M1 and M2 macrophages in diet-induced obese mice. *Diabetes*. 58:2574–2582. http://dx.doi.org/10.2337/db08-1475

Galkina, E., A. Kadl, J. Sanders, D. Varughese, I.J. Sarembock, and K. Ley. 2006. Lymphocyte recruitment into the aortic wall before and during development of atherosclerosis is partially L-selectin dependent. *J. Exp. Med.* 203:1273–1282. http://dx.doi.org/10.1084/jem.20052205

Gallardo-Soler, A., C. Gómez-Nieto, M.L. Campo, C. Marathe, P. Tontonoz, A. Castrillo, and I. Corraliza. 2008. Arginase I induction by modified lipoproteins in macrophages: a peroxisome proliferator-activated receptor-gamma/delta-mediated effect that links lipid metabolism and immunity. *Mol. Endocrinol.* 22:1394–1402. http://dx.doi.org/10.1210/me.2007-0525

Gay, N.J., M. Gangloff, and L.A. O'Neill. 2011. What the Myddosome structure tells us about the initiation of innate immunity. *Trends Immunol.* 32:104–109. http://dx.doi.org/10.1016/j.it.2010.12.005

Haghighat, A., D. Weiss, M.K. Whalin, D.P. Cowan, and W.R. Taylor. 2007. Granulocyte colony-stimulating factor and granulocyte macrophage colony-stimulating factor exacerbate atherosclerosis in apolipoprotein E-deficient mice. *Circulation*. 115:2049–2054. http://dx.doi.org/10.1161/CIRCULATIONAHA.106.665570

Hamilton, J.A. 2008. Colony-stimulating factors in inflammation and autoimmunity. *Nat. Rev. Immunol.* 8:533–544. http://dx.doi.org/10.1038/nri2356

Hamilton, J.A., D. Myers, W. Jessup, F. Cochrane, R. Byrne, G. Whitty, and S. Moss. 1999. Oxidized LDL can induce macrophage survival, DNA synthesis, and enhanced proliferative response to CSF-1 and GM-CSF. *Arterioscler. Thromb. Vasc. Biol.* 19:98–105. http://dx.doi.org/10.1161/01.ATV.19.1.98

Harari, O.A., P. Alcaide, D. Ahl, F.W. Luscinskas, and J.K. Liao. 2006. Absence of TRAM restricts Toll-like receptor 4 signaling in vascular endothelial cells to the MyD88 pathway. *Circ. Res.* 98:1134–1140. http://dx.doi.org/10.1161/01.RES.0000220105.85182.28

Hatley, M.E., S. Srinivasan, K.B. Reilly, D.T. Bolick, and C.C. Hedrick. 2003. Increased production of 12/15 lipoxygenase eicosanoids accelerates monocyte/endothelial interactions in diabetic db/db mice. *J. Biol. Chem.* 278:25369–25375.

Hazen, S.L., and J.W. Heinecke. 1997. 3-Chlorotyrosine, a specific marker of myeloperoxidase-catalyzed oxidation, is markedly elevated in low density lipoprotein isolated from human atherosclerotic intima. *J. Clin. Invest.* 99:2075–2081. http://dx.doi.org/10.1172/JCI119379

Hazen, S.L., F.F. Hsu, K. Duffin, and J.W. Heinecke. 1996. Molecular chlorine generated by the myeloperoxidase-hydrogen peroxide-chloride system of phagocytes converts low density lipoprotein cholesterol into a family of chlorinated sterols. *J. Biol. Chem.* 271:23080–23088. http://dx.doi.org/10.1074/jbc.271.38.23080

Hazen, S.L., R. Zhang, Z. Shen, W. Wu, E.A. Podrez, J.C. MacPherson, D. Schmitt, S.N. Mitra, C. Mukhopadhyay, Y. Chen, et al. 1999. Formation of nitric oxide-derived oxidants by myeloperoxidase in monocytes: pathways for monocyte-mediated protein nitration and lipid peroxidation In vivo. *Circ. Res.* 85:950–958. http://dx.doi.org/10.1161/01.RES.85.10.950

Himes, R.W., and C.W. Smith. 2010. Tlr2 is critical for diet-induced metabolic syndrome in a murine model. *FASEB J.* 24:731–739. http://dx.doi.org/10.1096/fj.09-141929

Hirosumi, J., G. Tuncman, L. Chang, C.Z. Görgün, K.T. Uysal, K. Maeda, M. Karin, and G.S. Hotamisligil. 2002. A central role for JNK in obesity and insulin resistance. *Nature*. 420:333–336. http://dx.doi.org/10.1038/nature01137

Holvoet, P., D.H. Lee, M. Steffes, M. Gross, and D.R. Jacobs Jr. 2008. Association between circulating oxidized low-density lipoprotein and incidence of the metabolic syndrome. *JAMA*. 299:2287–2293. http://dx.doi.org/10.1001/jama.299.19.2287

Hosoi, T., S. Yokoyama, S. Matsuo, S. Akira, and K. Ozawa. 2010. Myeloid differentiation factor 88 (MyD88)-deficiency increases risk of diabetes in mice. *PLoS ONE*. 5:5. http://dx.doi.org/10.1371/journal.pone.0012537

Hotamisligil, G.S. 2006. Inflammation and metabolic disorders. *Nature*. 444:860–867. http://dx.doi.org/10.1038/nature05485

Hotamisligil, G.S., N.S. Shargill, and B.M. Spiegelman. 1993. Adipose expression of tumor necrosis factor-alpha: direct role in obesity-linked insulin resistance. *Science*. 259:87–91. http://dx.doi.org/10.1126/science.7678183

Hou, B., B. Reizis, and A.L. DeFranco. 2008. Toll-like receptors activate innate and adaptive immunity by using dendritic cell-intrinsic and -extrinsic mechanisms. *Immunity*. 29:272–282. http://dx.doi.org/10.1016/j.immuni.2008.05.016

Huber, S.A., P. Sakkinen, D. Conze, N. Hardin, and R. Tracy. 1999. Interleukin-6 exacerbates early atherosclerosis in mice. *Arterioscler. Thromb. Vasc. Biol.* 19:2364–2367. http://dx.doi.org/10.1161/01.ATV.19.10.2364

Itabe, H., T. Obama, and R. Kato. 2011. The Dynamics of Oxidized LDL during Atherogenesis. *J. Lipids*. 2011:418313. http://dx.doi.org/10.1155/2011/418313

Jager, J., T. Grémeaux, M. Cormont, Y. Le Marchand-Brustel, and J.F. Tanti. 2007. Interleukin-1beta-induced insulin resistance in adipocytes through down-regulation of insulin receptor substrate-1 expression. *Endocrinology*. 148:241–251. http://dx.doi.org/10.1210/en.2006-0692

Kang, Z., C.Z. Altuntas, M.F. Gulen, C. Liu, N. Giltiay, H. Qin, L. Liu, W. Qian, R.M. Ransohoff, C. Bergmann, et al. 2010. Astrocyte-restricted ablation of interleukin-17-induced Act1-mediated signaling ameliorates autoimmune encephalomyelitis. *Immunity*. 32:414–425. http://dx.doi.org/10.1016/j.immuni.2010.03.004

Kang, Z., S. Swaidani, W. Yin, C. Wang, J.L. Barlow, M.F. Gulen, K. Bulek, J.S. Do, M. Aronica, A.N. McKenzie, et al. 2012. Epithelial cell-specific Act1 adaptor mediates interleukin-25-dependent helminth expulsion through expansion of Lin(-)c-Kit(+) innate cell population. *Immunity*. 36:821–833. http://dx.doi.org/10.1016/j.immuni.2012.03.021

Kano, A., M.J. Wolfgang, Q. Gao, J. Jacoby, G.X. Chai, W. Hansen, Y. Iwamoto, J.S. Pober, R.A. Flavell, and X.Y. Fu. 2003. Endothelial cells require STAT3 for protection against endotoxin-induced inflammation. *J. Exp. Med.* 198:1517–1525. http://dx.doi.org/10.1084/jem.20030077

Karaskov, E., C. Scott, L. Zhang, T. Teodoro, M. Ravazzola, and A. Volchuk. 2006. Chronic palmitate but not oleate exposure induces endoplasmic reticulum stress, which may contribute to INS-1 pancreatic beta-cell apoptosis. *Endocrinology*. 147:3398–3407.

Kenny, E.F., and L.A. O'Neill. 2008. Signalling adaptors used by Toll-like receptors: an update. *Cytokine*. 43:342–349. http://dx.doi.org/10.1016/j.cyto.2008.07.010

Kiechl, S., E. Lorenz, M. Reindl, C.J. Wiedermann, F. Oberhollenzer, E. Bonora, J. Willeit, and D.A. Schwartz. 2002. Toll-like receptor 4 polymorphisms and atherogenesis. *N. Engl. J. Med.* 347:185–192. http://dx.doi.org/10.1056/NEJMoa012673

Kim, T.W., K. Staschke, K. Bulek, J. Yao, K. Peters, K.H. Oh, Y. Vandenburg, H. Xiao, W. Qian, T. Hamilton, et al. 2007. A critical role for IRAK4 kinase activity in Toll-like receptor-mediated innate immunity. *J. Exp. Med.* 204:1025–1036. http://dx.doi.org/10.1084/jem.20061825

Kim, D.H., D. Sandoval, J.A. Reed, E.K. Matter, E.G. Tolod, S.C. Woods, and R.J. Seeley. 2008. The role of GM-CSF in adipose tissue inflammation. *Am. J. Physiol. Endocrinol. Metab.* 295:E1038–E1046. http://dx.doi.org/10.1152/ajpendo.00061.2008

Kirii, H., T. Niwa, Y. Yamada, H. Wada, K. Saito, Y. Iwakura, M. Asano, H. Moriwaki, and M. Seishima. 2003. Lack of interleukin-1beta decreases the severity of atherosclerosis in ApoE-deficient mice. *Arterioscler. Thromb. Vasc. Biol.* 23:656–660. http://dx.doi.org/10.1161/01.ATV.0000064374.15232.C3

Kleemann, R., S. Zadelaar, and T. Kooistra. 2008. Cytokines and atherosclerosis: a comprehensive review of studies in mice. *Cardiovasc. Res.* 79:360–376. http://dx.doi.org/10.1093/cvr/cvn120

Klover, P.J., T.A. Zimmers, L.G. Koniaris, and R.A. Mooney. 2003. Chronic exposure to interleukin-6 causes hepatic insulin resistance in mice. *Diabetes*. 52:2784–2789. http://dx.doi.org/10.2337/diabetes.52.11.2784

Könner, A.C., and J.C. Brüning. 2011. Toll-like receptors: linking inflammation to metabolism. *Trends Endocrinol. Metab.* 22:16–23. http://dx.doi.org/10.1016/j.tem.2010.08.007

Kosteli, A., E. Sugaru, G. Haemmerle, J.F. Martin, J. Lei, R. Zechner, and A.W. Ferrante Jr. 2010. Weight loss and lipolysis promote a dynamic immune response in murine adipose tissue. *J. Clin. Invest.* 120:3466–3479. http://dx.doi.org/10.1172/JCI42845

Lacey, D.C., A. Achuthan, A.J. Fleetwood, H. Dinh, J. Roiniotis, G.M. Scholz, M.W. Chang, S.K. Beckman, A.D. Cook, and J.A. Hamilton. 2012. Defining GM-CSF- and macrophage-CSF-dependent macrophage responses by in vitro models. *J. Immunol.* 188:5752–5765. http://dx.doi.org/10.4049/jimmunol.1103426

Lafontan, M., and D. Langin. 2009. Lipolysis and lipid mobilization in human adipose tissue. *Prog. Lipid Res.* 48:275–297. http://dx.doi.org/10.1016/j.plipres.2009.05.001

Lagathu, C., L. Yvan-Charvet, J.P. Bastard, M. Maachi, A. Quignard-Boulangé, J. Capeau, and M. Caron. 2006. Long-term treatment with interleukin-1beta induces insulin resistance in murine and human adipocytes. *Diabetologia*. 49:2162–2173. http://dx.doi.org/10.1007/s00125-006-0335-z

Landin, K., P. Lönnroth, M. Krotkiewski, G. Holm, and U. Smith. 1990. Increased insulin resistance and fat cell lipolysis in obese but not lean women with a high waist/hip ratio. *Eur. J. Clin. Invest.* 20:530–535. http://dx.doi.org/10.1111/j.1365-2362.1990.tb01922.x

Lin, S.C., Y.C. Lo, and H. Wu. 2010. Helical assembly in the MyD88-IRAK4-IRAK2 complex in TLR/IL-1R signalling. *Nature*. 465:885–890. http://dx.doi.org/10.1038/nature09121

Lumeng, C.N., J.L. Bodzin, and A.R. Saltiel. 2007. Obesity induces a phenotypic switch in adipose tissue macrophage polarization. *J. Clin. Invest.* 117:175–184. http://dx.doi.org/10.1172/JCI29881

Lundberg, A.M., D.F. Ketelhuth, M.E. Johansson, N. Gerdes, S. Liu, M. Yamamoto, S. Akira, and G.K. Hansson. 2013. Toll-like receptor 3 and 4 signalling through the TRIF and TRAM adaptors in haematopoietic cells promotes atherosclerosis. *Cardiovasc. Res.* 99:364–373. http://dx.doi.org/10.1093/cvr/cvt033

McCullough, A.J. 2011. Epidemiology of the metabolic syndrome in the USA. *J. Dig. Dis.* 12:333–340. http://dx.doi.org/10.1111/j.1751-2980.2010.00469.x

Michelsen, K.S., M.H. Wong, P.K. Shah, W. Zhang, J. Yano, T.M. Doherty, S. Akira, T.B. Rajavashisth, and M. Arditi. 2004. Lack of Toll-like receptor 4 or myeloid differentiation factor 88 reduces atherosclerosis and alters plaque phenotype in mice deficient in apolipoprotein E. *Proc. Natl. Acad. Sci. USA*. 101:10679–10684. http://dx.doi.org/10.1073/pnas.0403249101

Miyazaki, T., J. Kurokawa, and S. Arai. 2011. AIMing at metabolic syndrome. -Towards the development of novel therapies for metabolic diseases via apoptosis inhibitor of macrophage (AIM).-. *Circ. J.* 75:2522–2531. http://dx.doi.org/10.1253/circj.CJ-11-0891

Monteiro, R., and I. Azevedo. 2010. Chronic inflammation in obesity and the metabolic syndrome. *Mediators Inflamm.* 2010:2010. http://dx.doi.org/10.1155/2010/289645

Morris, D.L., K.E. Oatmen, T. Wang, J.L. DelProposto, and C.N. Lumeng. 2012. CX3CR1 deficiency does not influence trafficking of adipose tissue macrophages in mice with diet-induced obesity. *Obesity (Silver Spring)*. 20:1189–1199. http://dx.doi.org/10.1038/oby.2012.7

Nagy, L., P. Tontonoz, J.G. Alvarez, H. Chen, and R.M. Evans. 1998. Oxidized LDL regulates macrophage gene expression through ligand activation of PPARgamma. *Cell*. 93:229–240. http://dx.doi.org/10.1016/S0092-8674(00)81574-3

Neels, J.G., and J.M. Olefsky. 2006. Inflamed fat: what starts the fire? *J. Clin. Invest*. 116:33–35. http://dx.doi.org/10.1172/JCI27280

Nguyen, M.T., S. Favelyukis, A.K. Nguyen, D. Reichart, P.A. Scott, A. Jenn, R. Liu-Bryan, C.K. Glass, J.G. Neels, and J.M. Olefsky. 2007. A subpopulation of macrophages infiltrates hypertrophic adipose tissue and is activated by free fatty acids via Toll-like receptors 2 and 4 and JNK-dependent pathways. *J. Biol. Chem*. 282:35279–35292. http://dx.doi.org/10.1074/jbc.M706762200

Nishimura, S., I. Manabe, and R. Nagai. 2009. Adipose tissue inflammation in obesity and metabolic syndrome. *Discov. Med*. 8:55–60.

Ohashi, K., J.L. Parker, N. Ouchi, A. Higuchi, J.A. Vita, N. Gokce, A.A. Pedersen, C. Kalthoff, S. Tullin, A. Sams, et al. 2010. Adiponectin promotes macrophage polarization toward an anti-inflammatory phenotype. *J. Biol. Chem*. 285:6153–6160. http://dx.doi.org/10.1074/jbc.M109.088708

Petrasek, J., A. Dolganiuc, T. Csak, B. Nath, I. Hritz, K. Kodys, D. Catalano, E. Kurt-Jones, P. Mandrekar, and G. Szabo. 2011. Interferon regulatory factor 3 and type I interferons are protective in alcoholic liver injury in mice by way of crosstalk of parenchymal and myeloid cells. *Hepatology*. 53:649–660. http://dx.doi.org/10.1002/hep.24059

Plomgaard, P., K. Bouzakri, R. Krogh-Madsen, B. Mittendorfer, J.R. Zierath, and B.K. Pedersen. 2005. Tumor necrosis factor-alpha induces skeletal muscle insulin resistance in healthy human subjects via inhibition of Akt substrate 160 phosphorylation. *Diabetes*. 54:2939–2945. http://dx.doi.org/10.2337/diabetes.54.10.2939

Podrez, E.A., M. Febbraio, N. Sheibani, D. Schmitt, R.L. Silverstein, D.P. Hajjar, P.A. Cohen, W.A. Frazier, H.F. Hoff, and S.L. Hazen. 2000. Macrophage scavenger receptor CD36 is the major receptor for LDL modified by monocyte-generated reactive nitrogen species. *J. Clin. Invest*. 105:1095–1108. http://dx.doi.org/10.1172/JCI8574

Prieur, X., C.Y. Mok, V.R. Velagapudi, V. Núñez, L. Fuentes, D. Montaner, K. Ishikawa, A. Camacho, N. Barbarroja, S. O'Rahilly, et al. 2011. Differential lipid partitioning between adipocytes and tissue macrophages modulates macrophage lipotoxicity and M2/M1 polarization in obese mice. *Diabetes*. 60:797–809. http://dx.doi.org/10.2337/db10-0705

Richards, M.R., A.S. Black, D.J. Bonnet, G.D. Barish, C.W. Woo, I. Tabas, L.K. Curtiss, and P.S. Tobias. 2013. The LPS2 mutation in TRIF is atheroprotective in hyperlipidemic low density lipoprotein receptor knockout mice. *Innate Immun*. 19:20–29. http://dx.doi.org/10.1177/1753425912447130

Rios, F.J., M.M. Koga, M. Ferracini, and S. Jancar. 2012. Co-stimulation of PAFR and CD36 is required for oxLDL-induced human macrophages activation. *PLoS ONE*. 7:e36632. http://dx.doi.org/10.1371/journal.pone.0036632

Rotter, V., I. Nagaev, and U. Smith. 2003. Interleukin-6 (IL-6) induces insulin resistance in 3T3-L1 adipocytes and is, like IL-8 and tumor necrosis factor-alpha, overexpressed in human fat cells from insulin-resistant subjects. *J. Biol. Chem*. 278:45777–45784. http://dx.doi.org/10.1074/jbc.M301977200

Seimon, T.A., M.J. Nadolski, X. Liao, J. Magallon, M. Nguyen, N.T. Feric, M.L. Koschinsky, R. Harkewicz, J.L. Witztum, S. Tsimikas, et al. 2010. Atherogenic lipids and lipoproteins trigger CD36-TLR2-dependent apoptosis in macrophages undergoing endoplasmic reticulum stress. *Cell Metab.* 12:467–482. http://dx.doi.org/10.1016/j.cmet.2010.09.010

Shaposhnik, Z., X. Wang, M. Weinstein, B.J. Bennett, and A.J. Lusis. 2007. Granulocyte macrophage colony-stimulating factor regulates dendritic cell content of atherosclerotic lesions. *Arterioscler. Thromb. Vasc. Biol*. 27:621–627. http://dx.doi.org/10.1161/01.ATV.0000254673.55431.e6

Shaul, M.E., G. Bennett, K.J. Strissel, A.S. Greenberg, and M.S. Obin. 2010. Dynamic, M2-like remodeling phenotypes of CD11c+ adipose tissue macrophages during high-fat diet—induced obesity in mice. *Diabetes*. 59:1171–1181. http://dx.doi.org/10.2337/db09-1402

Shi W., M.E. Haberland, M.L. Jien, D.M. Shih, and A.J. Lusis. Endothelial responses to oxidized lipoproteins determine genetic susceptibility to atherosclerosis in mice. *Circulation*. 2000. 102:75–81.

Shi, H., M.V. Kokoeva, K. Inouye, I. Tzameli, H. Yin, and J.S. Flier. 2006. TLR4 links innate immunity and fatty acid-induced insulin resistance. *J. Clin. Invest*. 116:3015–3025. http://dx.doi.org/10.1172/JCI28898

Smith, D.D., X. Tan, O. Tawfik, G. Milne, D.J. Stechschulte, and K.N. Dileepan. 2010. Increased aortic atherosclerotic plaque development in female apolipoprotein E-null mice is associated with elevated thromboxane A2 and decreased prostacyclin production. *J. Physiol. Pharmacol*. 61:309–316.

Staels, B. 2002. Cardiovascular biology: a cholesterol tether. *Nature*. 417:699–701. http://dx.doi.org/10.1038/417699a

Stienstra, R., L.A. Joosten, T. Koenen, B. van Tits, J.A. van Diepen, S.A. van den Berg, P.C. Rensen, P.J. Voshol, G. Fantuzzi, A. Hijmans, et al. 2010. The inflammasome-mediated caspase-1 activation controls adipocyte differentiation and insulin sensitivity. *Cell Metab.* 12:593–605. http://dx.doi.org/10.1016/j.cmet.2010.11.011

Su, X., L. Ao, Y. Shi, T.R. Johnson, D.A. Fullerton, and X. Meng. 2011. Oxidized low density lipoprotein induces bone morphogenetic protein-2 in coronary artery endothelial cells via Toll-like receptors 2 and 4. *J. Biol. Chem*. 286:12213–12220. http://dx.doi.org/10.1074/jbc.M110.214619

Subramanian, M., E. Thorp, G.K. Hansson, and I. Tabas. 2013. Treg-mediated suppression of atherosclerosis requires MYD88 signaling in DCs. *J. Clin. Invest*. 123:179–188. http://dx.doi.org/10.1172/JCI64617

Suganami, T., J. Nishida, and Y. Ogawa. 2005. A paracrine loop between adipocytes and macrophages aggravates inflammatory changes: role of free fatty acids and tumor necrosis factor alpha. *Arterioscler. Thromb. Vasc. Biol*. 25:2062–2068. http://dx.doi.org/10.1161/01.ATV.0000183883.72263.13

Suganami, T., K. Tanimoto-Koyama, J. Nishida, M. Itoh, X. Yuan, S. Mizuarai, H. Kotani, S. Yamaoka, K. Miyake, S. Aoe, et al. 2007. Role of the Toll-like receptor 4/NF-kappaB pathway in saturated fatty acid-induced inflammatory changes in the interaction between adipocytes and macrophages. *Arterioscler. Thromb. Vasc. Biol*. 27:84–91. http://dx.doi.org/10.1161/01.ATV.0000251608.09329.9a

Sun, K., C.M. Kusminski, and P.E. Scherer. 2011. Adipose tissue remodeling and obesity. *J. Clin. Invest*. 121:2094–2101. http://dx.doi.org/10.1172/JCI45887

Takeuchi, O., and S. Akira. 2002. MyD88 as a bottle neck in Toll/IL-1 signaling. *Curr. Top. Microbiol. Immunol*. 270:155–167.

Tordjman, K., C. Bernal-Mizrachi, L. Zemany, S. Weng, C. Feng, F. Zhang, T.C. Leone, T. Coleman, D.P. Kelly, and C.F. Semenkovich. 2001. PPARalpha deficiency reduces insulin resistance and atherosclerosis in apoE-null mice. *J. Clin. Invest*. 107:1025–1034. http://dx.doi.org/10.1172/JCI11497

Trujillo, M.E., S. Sullivan, I. Harten, S.H. Schneider, A.S. Greenberg, and S.K. Fried. 2004. Interleukin-6 regulates human adipose tissue lipid metabolism and leptin production in vitro. *J. Clin. Endocrinol. Metab.* 89:5577–5582. http://dx.doi.org/10.1210/jc.2004-0603

Tsujita, T., C. Morimoto, and H. Okuda. 1995. Mechanism of increase in basal lipolysis of enlarged adipocytes in obese animals. *Obes. Res.* 3(Suppl 5):633S–636S. http://dx.doi.org/10.1002/j.1550-8528.1995.tb00478.x

van Tits, L.J., R. Stienstra, P.L. van Lent, M.G. Netea, L.A. Joosten, and A.F. Stalenhoef. 2011. Oxidized LDL enhances pro-inflammatory responses of alternatively activated M2 macrophages: a crucial role for Krüppel-like factor 2. *Atherosclerosis*. 214:345–349. http://dx.doi.org/10.1016/j.atherosclerosis.2010.11.018

Verreck, F.A., T. de Boer, D.M. Langenberg, M.A. Hoeve, M. Kramer, E. Vaisberg, R. Kastelein, A. Kolk, R. de Waal-Malefyt, and T.H. Ottenhoff. 2004. Human IL-23-producing type 1 macrophages promote but IL-10-producing type 2 macrophages subvert immunity to (myco)bacteria. *Proc. Natl. Acad. Sci. USA*. 101:4560–4565. http://dx.doi.org/10.1073/pnas.0400983101

Vita, J.A., M.L. Brennan, N. Gokce, S.A. Mann, M. Goormastic, M.H. Shishehbor, M.S. Penn, J.F. Keaney Jr., and S.L. Hazen. 2004. Serum myeloperoxidase levels independently predict endothelial dysfunction in humans. *Circulation*. 110:1134–1139. http://dx.doi.org/10.1161/01.CIR.0000140262.20831.8F

Wajchenberg, B.L., M. Nery, M.R. Cunha, and M.E. Silva. 2009. Adipose tissue at the crossroads in the development of the metabolic syndrome,

inflammation and atherosclerosis. *Arq. Bras. Endocrinol. Metabol.* 53:145–150. http://dx.doi.org/10.1590/S0004-27302009000200005

Waldo, S.W., Y. Li, C. Buono, B. Zhao, E.M. Billings, J. Chang, and H.S. Kruth. 2008. Heterogeneity of human macrophages in culture and in atherosclerotic plaques. *Am. J. Pathol.* 172:1112–1126. http://dx.doi.org/10.2353/ajpath.2008.070513

Wärnberg, J., E. Nova, L.A. Moreno, J. Romeo, M.I. Mesana, J.R. Ruiz, F.B. Ortega, M. Sjöström, M. Bueno, and A. Marcos; AVENA Study Group. 2006. Inflammatory proteins are related to total and abdominal adiposity in a healthy adolescent population: the AVENA Study. *Am. J. Clin. Nutr.* 84:505–512.

Weisberg, S.P., D. McCann, M. Desai, M. Rosenbaum, R.L. Leibel, and A.W. Ferrante Jr. 2003. Obesity is associated with macrophage accumulation in adipose tissue. *J. Clin. Invest.* 112:1796–1808. http://dx.doi.org/10.1172/JCI200319246

Wolfs, I.M., M.M. Donners, and M.P. de Winther. 2011. Differentiation factors and cytokines in the atherosclerotic plaque micro-environment as a trigger for macrophage polarisation. *Thromb. Haemost.* 106:763–771. http://dx.doi.org/10.1160/TH11-05-0320

Xu, H., G.T. Barnes, Q. Yang, G. Tan, D. Yang, C.J. Chou, J. Sole, A. Nichols, J.S. Ross, L.A. Tartaglia, and H. Chen. 2003. Chronic inflammation in fat plays a crucial role in the development of obesity-related insulin resistance. *J. Clin. Invest.* 112:1821–1830. http://dx.doi.org/10.1172/JCI200319451

Yao, J., T.W. Kim, J. Qin, Z. Jiang, Y. Qian, H. Xiao, Y. Lu, W. Qian, M.F. Gulen, N. Sizemore, et al. 2007. Interleukin-1 (IL-1)-induced TAK1-dependent Versus MEKK3-dependent NFkappaB activation pathways bifurcate at IL-1 receptor-associated kinase modification. *J. Biol. Chem.* 282:6075–6089. http://dx.doi.org/10.1074/jbc.M609039200

Zeyda, M., and T.M. Stulnig. 2007. Adipose tissue macrophages. *Immunol. Lett.* 112:61–67. http://dx.doi.org/10.1016/j.imlet.2007.07.003

Zeyda, M., K. Gollinger, E. Kriehuber, F.W. Kiefer, A. Neuhofer, and T.M. Stulnig. 2010. Newly identified adipose tissue macrophage populations in obesity with distinct chemokine and chemokine receptor expression. *Int J Obes (Lond).* 34:1684–1694. http://dx.doi.org/10.1038/ijo.2010.103

Zhang, R., M.L. Brennan, X. Fu, R.J. Aviles, G.L. Pearce, M.S. Penn, E.J. Topol, D.L. Sprecher, and S.L. Hazen. 2001. Association between myeloperoxidase levels and risk of coronary artery disease. *JAMA.* 286:2136–2142. http://dx.doi.org/10.1001/jama.286.17.2136

Zhu, S.N., M. Chen, J. Jongstra-Bilen, and M.I. Cybulsky. 2009. GM-CSF regulates intimal cell proliferation in nascent atherosclerotic lesions. *J. Exp. Med.* 206:2141–2149. http://dx.doi.org/10.1084/jem.20090866

Zieske, A.W., R.P. Tracy, C.A. McMahan, E.E. Herderick, S. Homma, G.T. Malcom, H.C. McGill Jr., and J.P. Strong; Pathobiological Determinants of Atherosclerosis in Youth Research Group. 2005. Elevated serum C-reactive protein levels and advanced atherosclerosis in youth. *Arterioscler. Thromb. Vasc. Biol.* 25:1237–1243. http://dx.doi.org/10.1161/01.ATV.0000164625.93129.64